35 Weisenburger DD, Nathwani BN, Winberg CD, Rappaport H. Multicentric angiofollicular lymph node hyperplasia: A clinicopathologic study of 16 cases. *Hum Pathol* 1985; **16**: 162–72.
36 Kumari P, Schechter GP, Saini N, Benator DA. Successful treatment of human immunodeficiency virus-related Castleman's disease with interferon-alpha. *Clin Infect Dis* 2000; **31**: 602–4.
37 Nishimoto N, Sasai M, Shima Y *et al.* Improvement in Castleman's disease by humanized anti-interleukin-6 receptor antibody therapy. *Blood* 2000; **95**: 56–61.
38 Nishimoto N, Kanakura Y, Aozasa K *et al.* Humanized anti-interleukin-6 receptor antibody treatment of multicentric Castleman disease. *Blood* 2005; **106**: 2627–32.
39 Beck JT, Hsu SM, Wijdenes J *et al.* Brief report: Alleviation of systemic manifestations of Castleman's disease by monoclonal anti-interleukin-6 antibody. *N Engl J Med* 1994; **330**: 602–5.
40 Gholam D, Vantelon JM, Al-Jijakli A, Bourhis JH. A case of multicentric Castleman's disease associated with advanced systemic amyloidosis treated with chemotherapy and anti-CD20 monoclonal antibody. *Ann Hematol* 2003; **82**: 766–8.
41 Hall PA, Donaghy M, Cotter FE, Stansfeld AG, Levison DA. An immunohistological and genotypic study of the plasma cell form of Castleman's disease. *Histopathology* 1989; **14**: 333–46; discussion 429–32.
42 Casper C, Nichols WG, Huang ML, Corey L, Wald A. Remission of HHV-8 and HIV-associated multicentric Castleman disease with ganciclovir treatment. *Blood* 2004; **103**: 1632–4.
43 Northfelt DW, Dezube BJ, Thommes JA *et al.* Pegylated-liposomal doxorubicin versus doxorubicin, bleomycin, and vincristine in the treatment of AIDS-related Kaposi's sarcoma: Results of a randomized phase III clinical trial. *J Clin Oncol* 1998; **16**: 2445–51.
44 Nunez M, Machuca A, Soriano V, Podzamczer D, Gonzalez-Lahoz J. Clearance of human herpesvirus type 8 viraemia in HIV-1-positive patients with Kaposi's sarcoma treated with liposomal doxorubicin. Caelyx/KS Spanish Study Group. *AIDS* 2000; **14**: 913–19.
45 Bollen J, Polstra A, Van Der Kuyl A *et al.* Multicentric Castleman's disease and Kaposi's sarcoma in a cyclosporin treated, HIV-1 negative patient: Case report. *BMC Blood Disord* 2003; **3**: 3.

Potential role of natural killer cells in controlling growth and infiltration of AIDS-associated primary effusion lymphoma cells

Md. Zahidunnabi Dewan,[1,2] Hiroshi Terunuma,[3,4] Masakazu Toi,[5] Yuetsu Tanaka,[6] Harutaka Katano,[7] Xuewen Deng,[3] Hiroyuki Abe,[4] Tadashi Nakasone,[2] Naoki Mori,[8] Tetsutaro Sata[7] and Naoki Yamamoto[1,2,9]

[1]Department of Molecular Virology, Graduate School, Tokyo Medical and Dental University, 1-5-45 Yushima, Bunkyo-ku, Tokyo 113-8519; [2]AIDS Research Center, National institute of Infectious Disease, 1-23-1 Toyama, Shinjuku-ku, Tokyo 162-8640; [3]Biotherapy Institute of Japan, 2-4-8 Edagawa, Koutou-ku, Tokyo 135-0051; [4]Kudan Clinic, 1-9-5 Kudankita, Chiyoda-ku, Tokyo 102-0073; [5]Division of Clinical Trials and Research, Breast Cancer Research and Treatment Program, Tokyo Metropolitan Komagome Hospital, Tokyo Medical Center for Cancer and Infectious Disease, 3-18-22 Honkomagome, Bunkyo-ku, Tokyo 113-8677; [6]Department of Immunology, Faculty of Medicine, University of the Ryukyus, 207 Uehara, Nishihara, Okinawa 903-0215; [7]Department of Pathology, National Institute of Infectious Diseases, 1-23-1 Toyama, Shinjyuku-ku, Tokyo 162-8640; [8]Division of Molecular Virology and Oncology, Graduate School of Medicine, University of the Ryukyus, 207 Uehara, Nishihara, Okinawa 903-0215, Japan

(Received June 20, 2006/Revised August 3, 2006/Accepted August 4, 2006/Online publication September 25, 2006)

Natural killer (NK) cells are an important component of the innate immune response against microbial infections and tumors. Direct involvement of NK cells in tumor growth and infiltration has not yet been demonstrated clearly. Primary effusion lymphoma (PEL) cells were able to produce tumors and ascites very efficiently with infiltration of cells in various organs of T-, B- and NK-cell knock-out NOD/SCID/γc^{null} (NOG) mice within 3 weeks. In contrast, PEL cells formed small tumors at inoculated sites in T- and B-cell knock-out NOD/SCID mice with NK-cells while completely failing to infiltrate into various organs. Immunosupression of NOD/SCID by treatment with an antimurine TM-β1 antibody, which transiently abrogates NK cell activity *in vivo*, resulted in enhanced tumorigenicity and organ infiltration in comparison with non-treated NOD/SCID mice. Activated human NK cells inhibited tumor growth and infiltration in NOG mice. Our results suggest that NK cells play an important role in growth and infiltration of PEL cells, and activated NK cells could be a promising immunotherapeutic tool against tumor or virus-infected cells either alone or in combination with conventional therapy. The rapid and efficient engraftment of PEL cells in NOG mice also suggests that this new animal model could provide a unique opportunity to understand and investigate the mechanism of pathogenesis and malignant cell growth. (*Cancer Sci* 2006; 97: 1381–1387)

Primary effusion lymphoma (PEL) was originally identified in AIDS-associated immunodeficient patients and has been recognized by the World Health Organization as a distinct AIDS-related form of B-cell lymphoproliferative disorder.[1–3] PEL is a non-Hodgkin's type lymphoma derived from postgerminal center B cells.[4] The tumor clone is characteristically infected by the Kaposi's sarcoma-associated herpesvirus, formerly called human herpesvirus type 8 (HHV-8),[5] and most cases are coinfected with Epstein–Barr virus.[6,7] PEL shows a peculiar presentation involving lymphomatous effusions of serous cavities and only occasionally presents with a definable mass.[5]

Immunodeficient mouse models of human malignancy have contributed significantly to understanding the pathogenesis of diseases as well as therapeutic purpose. The congenitally athymic and hairless nude mouse lacking functional T cells has been utilized as a host for human xenotransplantations for 30 years.[8] Thereafter, severe combined immunodeficiency (SCID) mice were found to have a genetic defect preventing functional development of T and B lymphocytes,[9,10] and can be engrafted successfully with a variety of normal hematopoietic and neoplastic cells.[11,12] In comparison with conventional SCID, the NOD-SCID strain appears to be more promising as a tool for xenotransplantion of human tumors. However, the NOD-SCID mouse strain retains natural killer (NK) cell activity, macrophage function, complement activity and functional dendritic cells.[13] NK cells might play an important role in the rejection of implanted tissues or cells in SCID mice.[14–17] Although several models using mainly conventional nude and SCID mice are available, there are some major drawbacks: the requirement of long time periods, repeated transplantation, total body irradiation of mice, hormone supplements, etoposide pretreatment and anti-NK monoclonal antibodies required for tumor formation. These problems appear to hinder wider use of these animal models. Due to the low engraftment efficiency of hematopoietic and tumor cells transplanted in SCID mice, T, B and NK knock-out NOD/SCID/γc^{null} (NOG) mice were used in the present study to investigate the role of NK in tumor growth and metastasis.[13]

Natural killer cells are a type of lymphocyte that comprises up to 15% of peripheral blood lymphocytes and mediates innate immunity against pathogens and tumors.[17] In addition, NK cells are an important source of cytokines that regulate hematopoiesis and link the innate to the adaptive immune response through a bidirectional cross-talk with dendritic cells.[18,19] NK cells were originally discovered because of their ability to kill tumor and virally infected cells *in vitro*. NK-cell activity against these *in vitro* targets is spontaneous; it is readily apparent in individuals who have not been previously exposed to the target cell antigens. A clear involvement of NK cells in antitumor immunity *in vivo*, and the involvement of major histocompatibility complex (MHC) class I in NK-cell recognition, was shown in 1986 by Karre and colleagues.[20] They showed that the RMA T-cell lymphoma, derived from the Rauscher virus-induced murine cell line RBL-5, grew progressively in syngenic mice, but that an MHC class I-negative variant, RMA-S, was rejected by host NK cells. In many different situations, NK cells were shown to kill certain tumor cell lines *in vitro*, despite significant levels of MHC class I on their cell surface.[21,22] This implied that killing of MHC class I$^+$ tumor cells was mediated by activating receptors that were either not impaired by the inhibitory NK receptors for MHC class I or provided sufficient stimulation to overcome the negative regulation.

One cohort study showed that individuals with low natural cytotoxic activity of peripheral blood lymphocytes are at a

[9]To whom correspondence should be addressed. E-mail: yamamoto.mmb@tmd.ac.jp

doi: 10.1111/j.1349-7006.2006.00319.x

significantly higher risk of cancer, compared with those of median or high activity.[23] It has been reported recently that NK cells isolated from HIV-infected individuals are impaired in their ability to kill the virus-infected autologous cells, as well as tumor cell lines.[24–27] Previous studies also reported that NK-cell activity controls PEL and Kaposi's sarcoma (KS) development associated with HHV-8 infection.[28,29] The ability of the NK cells to kill relevant targets, such as tumor or virally infected cells, depends on the delicate balance of the patterns of expression of MHC class I-specific inhibitory NK receptors and activating receptors.[30,31] As there is no animal model in which NK-cell activities are genetically and selectively deficient to rule out the function of NK cells in viral infection and tumor growth and metastasis, most studies have relied on depleting NK cells in mice using monoclonal or polyclonal antibodies.[32,33] Depletion of NK cells *in vivo* by anti-NK antibody leads to enhanced tumor formation in several mouse tumor models.[15,34] Therefore, the role of NK cells in the course of tumor growth and infiltration as well as viral infection remains one of the major topics in tumor immunology.

In the present study, we investigated the direct involvement of NK cells in growth and infiltration of PEL cells using T, B and NK knock-out NOG mice,[13,35,36] and T and B knock-out NOD/SCID mice. NK knock-out NOG mice were most efficient in the formation of large tumors, massive ascites and infiltration within 3 weeks in comparison with NK-bearing NOD/SCID mice. We also provide evidence that activated human NK cells inhibit tumor growth and infiltration in NOG mice. These results suggest that NK cells play an important role in tumor growth and infiltration, and activated NK cells could be a promising immunotherapeutic strategy against AIDS-associated PEL or other malignancies either alone or in combination with conventional therapy.

Materials and Methods

Mice and inoculation of cell lines. NOG and NOD/SCID mice were obtained from the Central Institute for Experimental Animals (Kawasaki, Japan). All mice were maintained under specific pathogen-free conditions at the Animal Center of Tokyo Medical and Dental University (Tokyo, Japan). The Ethical Review Committee of the institute approved the experimental protocol.

Primary effusion lymphoma cell lines BCBL-1[37] and TY-1,[38] NK cell line KHYG-1 and bcr-abl$^+$ leukemic cell line K562 were cultured in RPMI-1640 medium supplemented with 2% heat-inactivated fetal bovine serum (FBS; JRH Biosciences, Lenexa, KS, USA), 100 U/mL penicillin and 10 μg/mL streptomycin. BCBL-1 and TY-1 cells were washed twice with serum-free RPMI-1640 and resuspended in fresh RPMI-1640. Mice were anesthetized with ether and cells were inoculated either subcutaneously (sc) in the postauricular region or intraperitoneally (ip) in the abdominal region of mice at doses of 1×10^7 and 2×10^6 cells per mouse, respectively. BCBL-1 cells were also inoculated either sc in the postauricular region or ip in the abdominal region of NOD/SCID mice with or without pretreatment with TMβ1 antibody, or in NOG mice. All mice were killed 3 weeks after inoculation with PEL cells. We measured tumor size, collected ascites from the abdomen of mice, and measured the volume of ascites.

Isolation and culture of NK cells. Blood was collected after obtaining informed consent from healthy volunteers. Peripheral blood mononuclear cells (PBMC) were isolated from the blood by Ficoll-Hypaque gradient centrifugation (Amersham Biosciences, Uppsala, Sweden), washed twice with RPMI-1640, and the number of cells counted. To generate activated NK cells, PBMC were cultured in anti-CD16-coated flasks with AIM-V medium (Invitrogen, Tokyo, Japan) supplemented with 5% auto-plasma, 700 U/mL interleukin (IL)-2 (Chiron, Amsterdam, the Netherlands), and 1 μL/mL OK432 (Chugai Pharmaceutical, Tokyo, Japan) for 24 h at 39°C, and then the cultured cells were centrifuged at 550 *g* for 10 min and the supernatants were discarded. Cells were again cultured in anti-CD16-uncoated flasks with AIM-V medium supplemented with 5% auto-plasma, and 700 U/mL IL-2 at 37°C for 2–3 weeks. During culture periods, we added medium several times for expansion and maintenance of activated NK cells. The purity of NK cells was 92–95%.

Flow cytometric analysis and cytotoxic activity. For five-color flow cytometric analysis (Cytomics FC500; Beckman Coulter, Miami, FL, USA), freshly isolated and activated NK cells were stained with monoclonal antibodies (ECD-labeled anti-CD3, PC5-labeled anti-CD4, PC7-labeled anti-CD8, PC7-labeled anti-CD16, PE or PC7-labeled anti-CD45, PC5-labeled anti-CD56, and PE-labeled anti-CD69 [Immunotech, Marseile, France]) and appropriate anti-isotypic monoclonal antibodies stained as negative controls. Data were analyzed by using CXP Analysis software version 1.1.

Freshly isolated and activated NK cells were tested for cytotoxic activity at various effector-to-target (E/T) ratios in a calcein-AM release assay using TERASCAN VP (Minerva Tech., Tokyo, Japan). We labeled the target cells with the immunofluorescent dye Calcein-AM solution (Do Jindo Laboratory, Kumamoto, Japan) and incubated them for 30 min. The cells were then washed with phosphate-buffer saline (PBS)(–) and the fluorescence intensity checked. Target cells and effector cells were suspended in RPMI-1640 with 10% FBS at various E/T ratios, added into 96-well plates and incubated for 2 h, and the fluorescence intensity was again checked.

Inoculation of activated NK cells into mice and collection of samples. Mice were inoculated with BCBL-1 (2×10^6) cells ip in the abdominal region of NOG mice. Three days after inoculation of PEL cells, mice were treated with either RPMI-1640 (control mice) or activated NK cells (1×10^7) ip on days 4, 10 and 17. All mice were killed 3 weeks after inoculation with PEL cells. We measured tumor size, collected ascites from the abdomen of mice, and measured the volume of ascites. Tissues and various organs of mice were also collected and fixed with 10% buffered formalin (Streck Tissue Fixative, Omaha, NE, USA), then processed to paraffin-embedded sections for staining with hematoxylin and eosin (HE) and immunostaining.

Immunohistochemistry. Paraffin sections of various organs were deparaffinized and hydrated in xylene or clearing agents and a graded alcohol series, then rinsed for 5 min in water. Deparaffinized samples were incubated with 0.025% trypsin/PBS for 30 min followed by washing, and then incubated with 0.3% H_2O_2 in methanol for 30 min at room temperature before being washed twice with PBS. Immunostaining was done for PEL cells with a 1:500 dilution of primary rabbit polyclonal antibody specific for HHV-8-encoded LANA.[39] This was followed by washing in PBS and incubation with a secondary antibody, biotinylated antirabbit IgG, after which cells were again washed in PBS and incubated with horseradish peroxidase-conjugated streptavidin for 30 min at room temperature. After two washes in PBS, the amplification procedure was carried out using kits according to the manufacturer's instructions (catalyzed signal amplification system kit; DAKO, Copenhagen, Denmark). The signal was visualized using 0.2 mg/mL diaminobenzidine and 0.015% H_2O_2 in 0.05 M Tris-HCl, pH 7.6. Positive staining was visualized after incubation of these samples with a mixture of 0.05% 3,3′-diaminobenzidine tetrahydrochloride in 50 mM Tris-HCl buffer and 0.01% H_2O_2 for 5 min. The samples were counterstained with hematoxylin for 2 min, dehydrated completely, cleaned in xylene and then mounted. HE and immunostaining were visualized and photographed under light microscopy (BX41 and DP70; Olympus, Tokyo, Japan).

doi: 10.1111/j.1349-7006.2006.00319.x

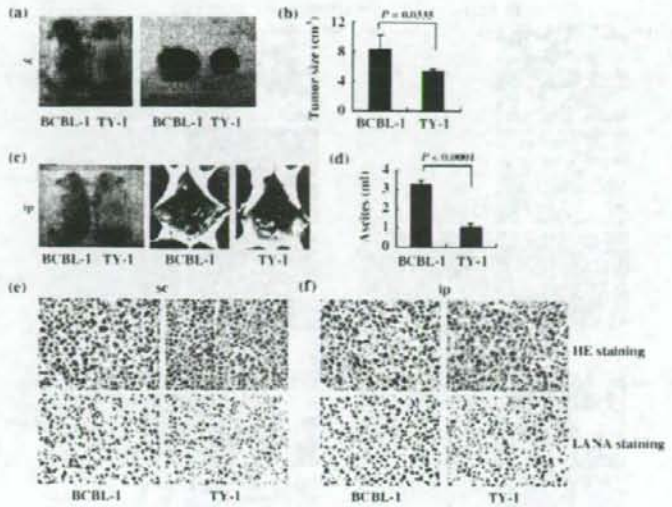

Fig. 1. Successful engraftment and tumor marker of primary effusion lymphoma (PEL) cells in T, B and natural killer (NK) knock-out NOG mice. (a) Photograph of mice inoculated with BCBL-1 and TY-1 cells subcutaneously in the postauricular region (left panel) and those of subcutaneously formed BCBL-1 and TY-1 tumor 3 weeks after inoculation of cells (right panel). (b) Subcutaneous tumor size of mice inoculated with BCBL-1 and TY-1 cells, shown as the mean ± s.e.m. from five mice ($P = 0.0335$). (c) Photograph of ascites-bearing mice inoculated with BCBL-1 and TY-1 cells intraperitonealy in the abdominal region (left panel) and peritoneal cavity of mice 21 days after inoculation of BCBL-1 (middle panel) and TY-1 cells (right panel). Arrow head indicates the tumor in mice inoculated intraperitonealy. (d) Volume of ascites in mice inoculated with various BCBL-1 and TY-1 cells, shown as the mean ± s.e.m. from five mice ($P < 0.0001$). (e,f) Hematoxylin–eosin (HE) and immunohistochemical staining of tumor tissue of BCBL-1 and TY-1 cells injected mice. Upper panels represent HE staining. Immunohistochemical staining was conducted using rabbit anti-LANA (lower panels). Left and right panels represent results with BCBL-1 and TY-1, respectively (magnification, ×40). Data are from (e) mice inoculated subcutaneously and (f) mice inoculated intraperitonealy.

Statistical analysis. The statistical analysis was carried out using StatView J-4.5 (Hulinks, Tokyo, Japan).

Results

Rapid tumor and massive ascites formation and infiltration of PEL cells in T, B and NK knock-out NOG mice. To investigate *in vivo* growth, PEL cell lines (BCBL-1 and TY-1) were inoculated sc in the postauricular region of NOG mice (Fig. 1a,b). Mice inoculated with cell lines BCBL-1 and TY-1 produced a visible tumor within 3 weeks in all NOG mice. The BCBL-1 cell line was very efficient in the formation of a large tumor (Fig. 1a,b), as well as development of clinical signs of near-death, such as pilorection, weight loss and cachexia in mice at the time of killing. The average tumor size in NOG mice inoculated with BCBL-1 and TY-1 was 8.25 cm^3 and 5.43 cm^3, respectively. PEL is an AIDS-associated non-Hodgkin's lymphoma that is characterized by lymphomatous effusions of serous cavities and rarely presents with a definable tumor mass.[5,7] To establish a clinically relevant PEL model, we inoculated BCBL-1 and TY-1 cells ip in the abdominal region of NOG mice (Fig. 1c,d). BCBL-1 and TY-1 produced massive ascites and a small tumor mass in the peritoneal cavity within 3 weeks of inoculation in all mice. The BCBL-1 cell line was most efficient in the formation of massive ascites (Fig. 1c,d), as well as development of clinical signs of near-death. The average volume of ascites in NOG mice inoculated with BCBL-1 and TY-1 was 3.26 mL and 1.05 mL, respectively. To test whether tumors maintain original histomorphology and expression patterns of tumor markers in NOG, we carried out HE and immunostaining of tumor tissues and various organs obtained from mice inoculated with BCBL-1 and TY-1 cells. Histological and immunological analysis revealed that *in vivo* tumor cells had well-preserved morphology as well as expression of the viral gene *LANA* (Fig. 1e,f). These results show that PEL cell lines inoculated either sc into the postauricular region or ip in the abdominal region of NOG mice were able to produce a large tumor and ascites very efficiently. Interestingly, ip-inoculated PEL cells were found to form clinically relevant lymphomatous effusions in the peritoneal cavity as well as a small definable mass.

To assess the tissue distribution of PEL cells, we carried out histological examinations of the different organs of NOG mice after inoculation of the cells. Infiltration of tumor cells was found not only in primary tumor tissues, but also to a lesser extent in the lung of NOG mice inoculated sc with BCBL-1 and TY-1 (Fig. 2a,b). We found that mice inoculated ip with BCBL-1 cells exhibited infiltration in the lung, liver and spleen (Fig. 2c), whereas TY-1 cells did so to a lesser extent only in the lung and liver (Fig. 2d). HE and immunohistochemical staining showed a degree of infiltration of tumor cells at the site of inoculation and various organs with BCBL-1 and TY-1 (Fig. 2). Furthermore, BCBL-1 was most efficient at infiltrating the lung (Fig. 2a,c). Interestingly, ip-inoculated PEL cells appeared to infiltrate various organs of mice more aggressively and massively than sc inoculation. This extremely rapid tumor formation and infiltration in all mice is one of the hallmarks of our clinically relevant animal model without changes in histomorphology or tumor marker expression.

Role of NK cells in the growth and infiltration of PEL cell *in vivo*. Severe combined immunodeficiency mice lack functional T and B lymphocytes, but NK-cell activity remains normal.[10,17,40] Despite severe immunological defects, SCID mice have the ability to reject xenografts. Further, immunosupression of SCID by treatment with etoposide, irradiation or an anti-NK antibody, which transiently abrogates NK-cell activity *in vivo*, results in enhanced tumor growth in mice.[41–47] To determine the possibility that NK-cell activity suppresses tumorigenesis in conventional SCID mice, the PEL cell line BCBL-1 was inoculated either sc in the postauricular region or ip in the abdominal region of T and B knock-out NOD/SCID mice with or without pretreatment of with TMβ1 antibody, or T, B and NK knock-out NOG mice (Fig. 3a–g). BCBL-1 cells were able to produce tumors at inoculation sites in NOD/SCID mice with common γ-chain. Immunosupression of NOD/SCID by treatment with an antimurine TMβ1 antibody, which transiently abrogates natural killer cell activity *in vivo*, resulted in induction of larger tumor and ascites formation in comparison with non-treated NOD/SCID mice. NOG mice lacking common γ-chain inoculated with BCBL-1 cells were most efficient in the formation of large tumor and massive ascites within 3 weeks.

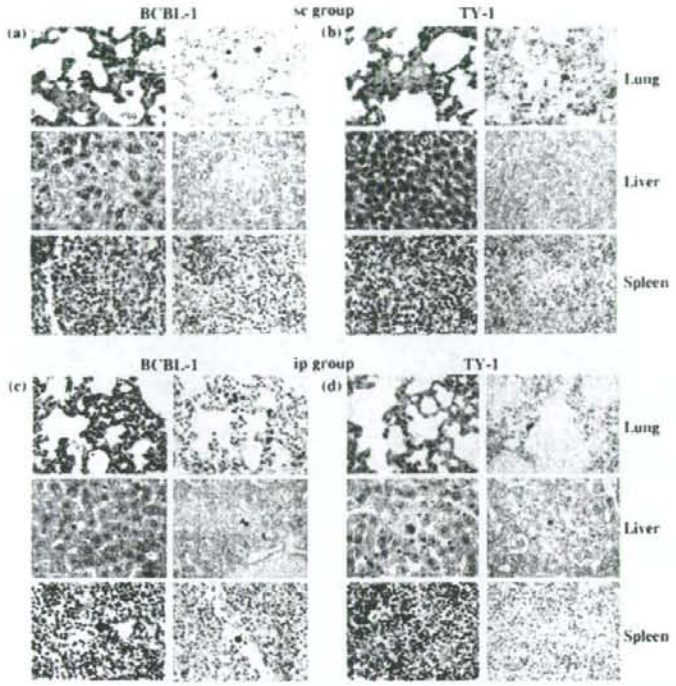

Fig. 2. Metastasis of primary effusion lymphoma (PEL) cells in various organs of T, B and natural killer (NK) knock-out NOG mice. (a–d) Histological analysis of lung, liver and spleen of mice inoculated with BCBL-1 and TY-1 cells either (a,b) subcutaneously (sc) or (c,d) intraperitonealy (ip). Immunohistochemical staining was conducted using anti-LANA. Data are from (a,c) BCBL-1-inoculated mice and (b,d) TY-1-inoculated mice. Left and right panels of all figures represent hematoxylin–eosin and immunostaining, respectively (magnification, ×40).

NOG mice have a defective common cytokine receptor, γ chain. Mutation in the common cytokine receptor γ chain leads to life-threatening, X-linked, severe combined immunodeficiency disease (XSCID) in humans, characterized by an extremely low number of T and NK cells.[48,49] These results suggest that NK cells are responsible for the formation of a progressively growing rapid large tumor and massive ascites of PEL cells in SCID mice at inoculation sites.

Severe combined immunodeficiency mice have NK cells, an important immune effector population implicated in protection against tumor metastasis and viral infection.[17,50] It has been reported recently that individuals with low natural cytotoxic activity of peripheral blood lymphocytes are at a significantly higher risk of cancer, compared with those of median or high activity, as well as functional impairment of NK cells in viral infection.[23] To assess the infiltration of PEL cells, we carried out histological examinations of tumor tissue and the different organs of mice inoculated with BCBL-1 cells (Fig. 3h). Infiltration of tumor cells was found in various organs of NOG mice inoculated with BCBL-1 cells. We found that NOD/SCID inoculated with BCBL-1 cells exhibited no infiltrate in any organs. NOD/SCID mice immunosuppressed by pretreatment with anti-NK antibody showed infiltration of PEL cells to a lesser extent in various organs of mice inoculated with BCBL-1 cells. HE and immunohistochemical staining showed a degree of infiltration of tumor cells in the lung of mice inoculated with BCBL-1 (Fig. 3h). These results suggest that NK cells play an important role in the infiltration of cancer cells in various organs.

Activated NK cells inhibit tumor growth and infiltration *in vivo*. As the above results suggested the potential role of NK cells in tumor growth and metastasis, we next examined whether adoptive transfer of activated NK cells could inhibit tumor growth and infiltration of xenografted PEL cells in the NOG mouse model. For this purpose, freshly isolated PBMC from the blood of healthy donors were cultured for 2–3 weeks to generate NK cells. NK cells were expanded *ex vivo* by several hundred to 2500-fold after 2 weeks cultivation and the expression level of CD69, an activated marker of NK cells, was increased dramatically. The purity of the activated NK cells used in the present study was 92–95% (data not shown). NK cells use cytoplasmic granules containing perforins and granzymes to kill the target cells. Using a highly sensitive flow cytometry-based intracellular cytokine assay, we next investigated the expression of intracellular perforins and granzymes in NK cells. Intracellular perforin and granzyme expression was increased in activated culture cells in comparison to freshly isolated cells from healthy donors (data not shown). PBMC, NK cell line KHYG-1 and activated NK cells were analyzed for cytotoxic activity against the NK-susceptible K562 erythroleukemia cell line (Fig. 4a,b). Cytotoxic activity of cells cultured for 2 weeks was increased significantly compared with freshly isolated PBMC from healthy donors (Fig. 4b). Activated NK cells also killed PEL cells efficiently *in vitro* at various E/T ratios, but the NK cell line KHYG-1 did not (Fig. 4c).

To examine the antitumor effect of activated NK cells against PEL, we injected the PEL cell line BCBL-1 (2×10^6) ip into the abdominal region of NOG mice. Three days after inoculation, mice were treated with either RPMI-1640 (as control) or activated NK cells (1×10^7) ip on days 4, 10 and 17. BCBL-1 cell inoculation promoted the development of massive ascites in the peritoneal cavity of all control mice within 3 weeks of inoculation. In contrast, activated NK-treated mice appeared to be

doi: 10.1111/j.1349-7006.2006.00319.x

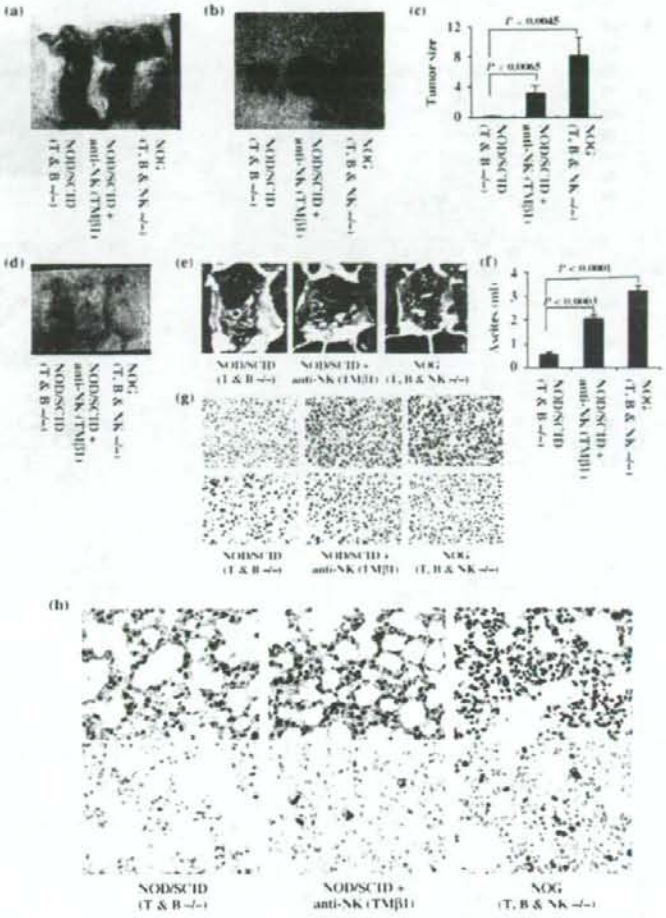

Fig. 3. Natural killer (NK) cells in tumor growth and infiltration. BCBL-1 cells were inoculated subcutaneously in the postauricular region or intraperitonealy in the abdominal region of T and B knock-out NOD/SCID, TMβ1-pretreated T and B knock-out NOD/SCID and T, B and NK knock-out NOG mice. (a) Photograph of mice inoculated with BCBL-1 cells subcutaneously in the postauricular region. (b) Photograph of BCBL-1 tumor 3 weeks formed subcutaneously after inoculation of cells. (c) Subcutaneous tumor size of mice inoculated with BCBL-1 cells, shown as the mean ± s.e.m. from six mice. Tumor size of TMβ1-pretreated NOD/SCID mice was significantly larger than NOD/SCID ($P = 0.0065$) and that of NOG mice was more significant than NOD/SCID ($P = 0.0045$). (d) Photograph of ascites-bearing mice inoculated with BCBL-1 cells intraperitonealy in the abdominal region. (e) Photograph of the peritoneal cavity of mice 3 weeks after inoculation of BCBL-1. Left, middle and right panels represent the T and B knock-out NOD/SCID, TMβ1-pretreated T and B knock-out NOD/SCID and T, B and NK knock-out NOG mice, respectively. Arrow head indicates the tumor in mice inoculated intraperitonealy. (f) Volume of ascites in mice inoculated with BCBL-1 cells, shown as the mean ± s.e.m. from six mice. Volume of ascites in TMβ1-pretreated NOD/SCID mice was significantly higher than NOD/SCID ($P = 0.0003$) and that of NOG mice was more significant than NOD/SCID ($P < 0.0001$). Hematoxylin–eosin (HE) and immunohistochemical staining of (g) lung tissue and (h) tumor tissue of BCBL-1-injected mice. Upper panels represent HE staining. Immunohistochemical staining was conducted using rabbit anti-LANA (lower panels). Left, middle and right panels represent results from T and B knock-out NOD/SCID, TMβ1-pretreated T and B knock-out NOD/SCID and T, B and NK knock-out NOG mice, respectively. Magnification, ×40.

healthy and had a significantly lower volume of ascites (Fig. 5a,b). Clinical evaluation of organ infiltration 3 weeks after injection of PEL cells showed that activated NK treatment inhibited their infiltration into the lung. In contrast, all control mice showed massive infiltration of tumor cells into the lung (Fig. 5c). Organ infiltration of tumor cells was analyzed and evaluated by HE and immunostaining of LANA. These data indicate that activated NK cells significantly inhibit the growth and infiltration of PEL cells *in vivo* (Fig. 5).

Discussion

Natural killer cells form a first line of defense against pathogens or host cells that are stressed or cancerous. To execute the concept of using activated NK cells in order to prevent cancer, it is indispensable to know how NK cells are important for tumor growth and infiltration. There have been a number of reports about the contribution of NK cells in tumor growth and metastasis. In particular, whole-body irradiation has been reported to suppress NK activity and increase the ability of human and murine tumors to be transplanted into SCID mice.[42–46] Treatment of mice with murine anti-NK antibody, which transiently inhibits NK-cell activity, results in efficient engraftment of tumor cells in SCID mice.[15,47] In the present study, we demonstrated the direct role of NK cells in tumor growth and metastasis using T, B and NK knock-out NOG and T and B knock-out NOD/SCID mice. PEL cells were able to produce a large tumor and massive ascites very efficiently at inoculated sites and infiltrate various organs in T, B and NK nock-out NOG mice. We found that T and B knock-out NOD/SCID mice inoculated with PEL cells formed small tumors and a lower volume of ascites, but completely failed to infiltrate. T and B knock-out NOD/SCID mice were further immunosuppressed by pretreatment with anti-NK antibody, which enhanced tumor and ascites formation as well as organ infiltration. These results demonstrate the critical role of NK cells in tumor growth and infiltration using NK knock-out mice. It is of particular importance that ip-inoculated PEL cells were found to form clinically relevant lymphomatous effusions in the peritoneal cavity and small tumor mass as well as infiltration. This clinically relevant

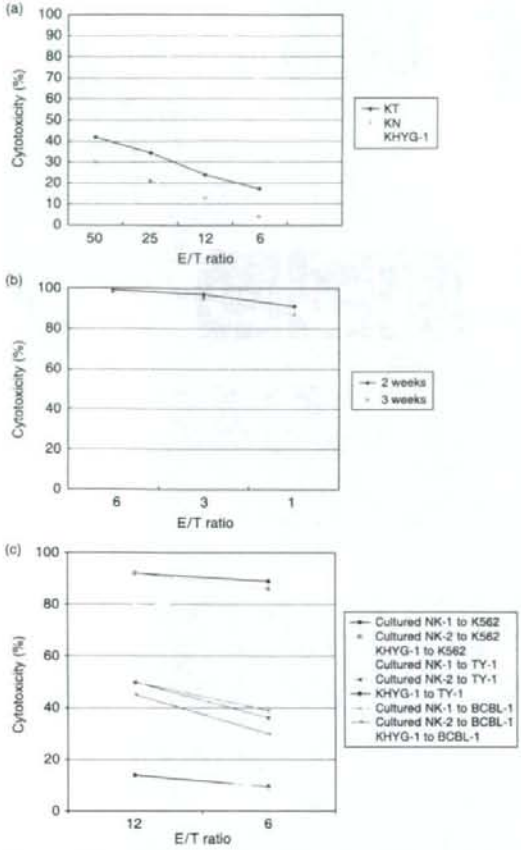

Fig. 4. Cytotoxic activity of activated natural killer (NK) *in vitro* culture cells. (a) Spontaneous cytotoxic activity of freshly isolated peripheral blood mononuclear cells (KT-1 and KN-2 represent samples from two donors) and NK cell line KHYG-1 against K-562 cells at different effector-to-target (E/T) ratios. (b) Cells cultured for 2 weeks against K-562 cells at different E/T ratios. (c) Cytotoxic activity of activated NK cells (NK-1 and NK-2 represent samples from two donors) against primary effusion lymphoma cells *in vitro* at various E/T ratios.

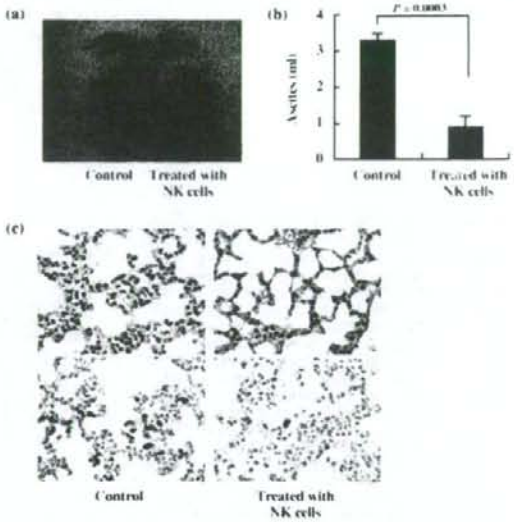

Fig. 5. Inhibition of primary effusion lymphoma (PEL) cell growth and infiltration in NOG mice. T, B and natural killer (NK) knock-out NOG mice were injected with PEL cells (2×10^6) intraperitonealy in the abdominal region. Mice were administered either RPMI-1640 or activated NK cells (1×10^7) intraperitonealy on days 4, 10 and 17 followed by observation for up to 3 weeks. (a) Photograph of ascites-bearing control PEL mice and activated NK-treated PEL mice. (b) Volume of ascites in control PEL mice and activated NK-treated PEL mice. Volume of ascites in mice inoculated with BCBL-1 cells, shown as the mean ± s.e.m. from six mice ($P = 0.0003$). (c) Hematoxylin–eosin (HE) and immunohistochemical staining of the lung of NOG mice 3 weeks after inoculation of PEL cells using anti-LANA. Upper and lower panels show HE and immunohistochemical staining, respectively. Left and right panels represent the data from control mice and mice treated with activated NK cells, respectively. Magnification, ×40. The data represent six mice in each group and three healthy donors (two mice for each donor).

animal model without changes in its histomorphology or tumor marker expression would be useful to understand and investigate the mechanism of PEL cell growth and infiltration.

In patients with cancer and viral infection, NK-cell function has been shown to be impaired, as determined by the reduced proliferation, response to interferon (IFN), and cytotoxicity of the cells of patients *ex vivo*.[51,52] In the present study, we inoculated activated NK cells to treat tumor-bearing mice to further clarify the role of NK cells in tumor growth and infiltration. Transfer of activated NK cells in T, B and NK knock-out NOG mice showed significant inhibition of tumor and ascites formation as well as infiltration. T, B and NK knock-out NOG mice treated with activated NK cells rejected the tumor cells to a similar extent as T and B knock-out NOD/SCID mice.

Natural killer cells kill target cells by various mechanisms. One way is by the release of cytoplasmic granules – complex organelles that combine specialized storage and secretory functions with the generic degradative functions of lysosomes. These granules contain a number of proteins, such as perforins and granzymes, which lyse target cells. Increased perforin and granzyme expression in activated NK cells was significantly correlated with inhibition of tumor growth and metastasis in the NOG mouse model. Perforin- and granzyme-mediated apoptosis is the principal pathway used by NK cells to eliminate tumor and virus-infected cells.[53] Studies in perforin-deficient mice have revealed that this protein is required for most NK-cell cytotoxicity.[54]

In summary, NK knock-out NOG mice were very efficient in the formation of primary tumors and organ infiltration. These results indicate that activated human NK cells prevent tumor growth and infiltration in NOG mice. Finally, our results suggest that NK cells play a critical role in tumor growth and infiltration, and that activated NK cells could be a promising immunotherapeutic strategy against cancer or viral infection either alone or in combination with conventional therapy. The reproducible growth behavior and preservation of characteristic features of PEL cells also suggest that the NOG mouse model system described in the present study may provide a novel opportunity to understand and investigate the mechanism of pathogenesis and malignant cell growth of PEL.

doi: 10.1111/j.1349-7006.2006.00319.x

Acknowledgments

We thank K. Ohba of the Department of Molecular Virology, S. Ichinose of the Instrumental Analysis Research Center and S. Endo of the Animal Research Center, Tokyo Medical and Dental University for their advice and assistance with the experiments. We also thank Y. Sato of the National Institute of Infectious Diseases for her excellent technical assistance. This work was supported by grants from the Ministry of Education, Science and Culture; the Ministry of Health, Labor and Welfare; and Human Health Science of Japan.

References

1 Jaffe ES, Harris NL, Stein H, Vardiman JW, eds. *World Health Organization Classification of Tumors, Pathology and Genetics of Tumors of Haematopoietic and Lymphoid Tissues*. Lyon, France: IARC Press, 2001.
2 Gaidano G, Carbone A. Primary effusion lymphoma: a liquid phase lymphoma of fluid-filled body cavities. *Adv Cancer Res* 2001; **80**: 115–46.
3 Cesarman E, Knowles DM. The role of Kaposi's sarcoma-associated herpesvirus (KSHV/HHV-8) in lymphoproliferative diseases. *Semin Cancer Biol* 1999; **9**: 165–74.
4 Klein U, Gloghini A, Gaidano G *et al*. Gene expression profile analysis of AIDS-related primary effusion lymphoma (PEL) suggests a plasmablastic derivation and identifies PEL-specific transcripts. *Blood* 2003; **102**: 4115–21.
5 Cesarman E, Chang Y, Moore PS, Said JW, Knowles DM. Kaposi's sarcoma-associated herpesvirus-like DNA sequences in AIDS-related body-cavity-based lymphomas. *N Engl J Med* 1995; **332**: 1186–91.
6 Horenstein MG, Nador RG, Chadburn A *et al*. Epstein–Barr virus latent gene expression in primary effusion lymphomas containing Kaposi's sarcoma-associated herpesvirus/human herpesvirus-8. *Blood* 1997; **90**: 1186–91.
7 Nador RG, Cesarman E, Chadburn A *et al*. Primary effusion lymphoma: a distinct clinicopathologic entity associated with the Kaposi's sarcoma-associated herpes virus. *Blood* 1996; **88**: 645–56.
8 Schmidt M, Deschner EE, Thaler HT, Clemments L, Good RA. Gastrointestinal cancer studies in the human to nude mouse heterotransplant system. *Gastroenterology* 1977; **72**: 829–37.
9 Bosma GC, Custer RP, Bosma MJ. A severe combined immunodeficiency mutation in the mouse. *Nature* 1983; **301**: 527–30.
10 Schuler W, Bosma MJ. Nature of the scid defect: a defective VDJ recombinase system. *Curr Top Microbiol Immunol* 1989; **152**: 55–62.
11 Kamel-Reid S, Letarte M, Sirard C *et al*. A model of human acute lymphoblastic leukemia in immune-deficient SCID mice. *Science* 1989; **246**: 1597–600.
12 Mosier DE, Gulizia RJ, Baird SM, Wilson DB. Transfer of a functional human immune system to mice with severe combined immunodeficiency. *Nature* 1988; **335**: 256–9.
13 Ito M, Hiramatsu H, Kobayashi K *et al*. NOD/SCID/γ_c^{null} mouse: An excellent recipient mouse model for engraftment of human cells. *Blood* 2002; **100**: 3175–82.
14 Dorshkind K, Pollack SB, Bosma MJ, Phillips RA. Natural killer (NK) cells are present in mice with severe combined immunodeficiency (scid). *J Immunol* 1985; **134**: 3798–801.
15 Feuer G, Stewart SA, Baird SM, Lee F, Feuer R, Chen ISY. Potential role of natural killer cells in controlling tumorigenesis by human T-cell leukemia Viruses. *J Virol* 1994; **69**: 1328–33.
16 Welsh RM. Regulation of virus infections by natural killer cells: a review. *Nat Immun Cell Growth Regul* 1986; **5**: 169–99.
17 Trinchieri G. Biology of natural killer cells. *Adv Immunol* 1989; **47**: 187–376.
18 Moretta A. Natural killer cells and dendritic cells: rendezvous in abused tissues. *Nat Rev Immunol* 2002; **2**: 957–64.
19 Raulet DH. Interplay of natural killer cells and their receptors with the adaptive immune response. *Nat Immunol* 2004; **5**: 996–1002.
20 Karre K, Ljungger HG, Piontek G, Kiessling R. Selective rejection of H-2-deficient lymphoma variants suggests alternative immune defense strategy. *Nature* 1986; **319**: 675–8.
21 Pena J, Alonso C, Solana R, Serrano R, Carracedo J, Ramirez R. Natural killer susceptibility is independent of HLA class I antigen expression on the cell lines obtained from human solid tumors. *Eur J Immunol* 1990; **20**: 2445–9.
22 Litwin V, Gumperz J, Parham P, Philips JH, Lanier LL. Specificity of HLA class I antigen recognition by human NK clones: evidence for clonal heterogeneity, protection by self and non-self alleles, and influence of the target cell type. *J Exp Med* 1993; **178**: 1321–36.
23 Imai K, Matsuyama S, Miyake S, Suga K, Nakachi K. Natural cytotoxic activity of peripheral-blood lymphocytes and cancer incidence: an 11-year follow-up study of a general population. *Lancet* 2000; **356**: 1795–9.
24 Ullum H, Gotzsche PC, Victor J, Dickmeiss E, Skinhoj P, Pedersen BK. Defective natural immunity: an early manifestation of human immunodeficiency virus infection. *J Exp Med* 1995; **182**: 789–99.
25 Ahmad R, Menezes J. Defective killing activity against gp120/41-expressing human erythroleukaemic K562 cell line by monocytes and natural killer cells from HIV-infected individuals. *AIDS* 1996; **10**: 143–9.
26 Scott-Algara D, Paul P. NK cells and HIV infection: lessons from other viruses. *Curr Mol Med* 2002; **2**: 757–68.
27 Bonaparte MI, Barker E. Inability of natural killer cells to destroy autologous HIV-infected T lymphocytes. *AIDS* 2003; **17**: 487–94.
28 Sirianni MC, Libi F, Campagna M *et al*. Downregulation of the major histocompatibility complex class I molecules by human herpesvirus type 8 and impaired natural killer cell activity in primary effusion lymphoma development. *Br J Haematol* 2005; **130**: 92–5.
29 Sirianni MC, Vincenzi L, Topino S *et al*. NK cell activity controls human herpesvirus 8 latent infection and is restored upon highly active antiretroviral therapy in AIDS patients with regressing Kaposi's sarcoma. *Eur J Immunol* 2002; **32**: 2711–20.
30 Lanier LL. NK cell receptors. *Annu Rev Immunol* 1998; **16**: 356–93.
31 Moretta A, Bottino C, Mingari MC, Biassoni R, Moretta L. What is a natural killer cell? *Nat Immunol* 2002; **3**: 6–8.
32 Koo GC, Dumont FJ, Tutt M, Hackett J Jr, Kumar V. The NK-1.1(–) mouse: a model to study differentiation of murine NK cells. *J Immunol* 1986; **137**: 3742–7.
33 Smyth MJ, Crowe NY, Godfrey DI. NK cells and NKT cells collaborate in host protection from methylcholanthrene-induced fibrosarcoma. *Int Immunol* 2001; **13**: 459–63.
34 Smyth MJ, Godfery DI, Trapani JA. A fresh look at tumor immunosurveillance and immunotherapy. *Nature* 2001; **2**: 293–9.
35 Dewan MZ, Terashima K, Taruishi M *et al*. Rapid tumor formation of human T-cell leukemia virus type 1-infected cell lines in novel NOD-SCID/γ_c^{null} mice: suppression by an inhibitor against NF-κB. *J Virol* 2003; **77**: 5286–94.
36 Dewan MZ, Uchihara JN, Terashima K *et al*. Efficient intervention of growth and infiltration of primary adult T-cell leukemia cells by an HIV protease inhibitor, ritonavir. *Blood* 2006; **107**: 716–24.
37 Renne R, Zhong W, Herndier B *et al*. Lytic growth of Kaposi's sarcoma-associated herpesvirus (human herpesvirus 8) in culture. *Nat Med* 1996; **2**: 342–6.
38 Katano H, Hoshino Y, Morishita Y *et al*. Establishing and characterizing a CD30-positive cell line harboring HHV-8 from a primary effusion lymphoma. *J Med Virol* 1999; **58**: 394–401.
39 Katano H, Sato Y, Kurata T, Mori S, Sata T. High expression of HHV-8-encoded ORF73 protein in spindle-shaped cells of Kaposi's sarcoma. *Am J Pathol* 1999; **155**: 47–52.
40 Dorshkind K, Pollack SB, Bosma MJ, Phillips RA. Natural killer (NK) cells are present in mice with severe combined immunodeficiency (scid). *J Immunol* 1985; **134**: 3798–801.
41 Visonneau S, Cesano A, Torosian MH, Miller EJ, Santoli D. Growth characteristics and metastatic properties of human breast cancer xenografts in immunodeficient mice. *Am J Pathol* 1998; **152**: 1299–311.
42 Cavacini LA, Giles-Komar J, Kennel M, Quinn A. Effect of immunosuppressive therapy on cytolytic activity of immunodeficient mice: implications for xenogeneic transplantation. *Cell Immunol* 1992; **144**: 296–310.
43 Hochman PS, Cudkowicz G, Dausset J. Decline of natural killer cell activity in sublethally irradiated mice. *J Natl Cancer Inst* 1978; **61**: 265–8.
44 Huang YW, Richardson JA, Tong AW, Zhang BQ, Stone MJ, Vitetta ES. Disseminated growth of a human multiple myeloma cell line in mice with severe combined immunodeficiency disease. *Cancer Res* 1993; **53**: 1392–6.
45 Lapidot T, Sirard C, Vormoor J *et al*. A cell initiating human acute myeloid leukaemia after transplantation into SCID mice. *Nature* 1994; **367**: 645–8.
46 Taghian A, Budach W, Zietman A, Freeman J, Gioioso D, Suit HD. Quantitative comparison between the transplantability of human and murine tumors into the brain of NCr/Sed-nu/nu nude and severe combined immunodeficient mice. *Cancer Res* 1993; **53**: 5018–21.
47 Tanaka T, Tsudo M, Karasuyama H *et al*. Novel monoclonal antibody against murine IL-2 receptor beta-chain: Characterization of receptor expression in normal lymphoid cells and EL-4 cells. *J Immunol* 1991; **147**: 2222–8.
48 Noguchi M, Yi H, Rosenblatt HM *et al*. Interleukin-2 receptor gamma chain mutation results in X-linked severe combined immunodeficiency in humans. *Cell* 1993; **73**: 147–57.
49 Puck JM, Deschenes SM, Porter JC *et al*. The interleukin-2 receptor gamma chain maps to Xq13.1 and is mutated in X-linked severe combined immunodeficiency, SCIDX1. *Hum Mol Genet* 1993; **2**: 1099–104.
50 Welsh RM. Regulation of virus infections by natural killer cells: a review. *Nat Immun Cell Growth Regul* 1986; **5**: 169–99.
51 Whiteside TL, Herberman RB. Role of human natural killer cells in health and disease. *Clin Diagn Laboratory Immunol* 1994; **1**: 125–33.
52 Whiteside TL, Vujanovic NL, Herberman RB. Natural killer cells and tumor therapy. *Curr Top Microbiol Immunol* 1998; **230**: 221–44.
53 Trapani JA, Davis J, Sutton VR, Smyth MJ. Proapoptotic functions of cytotoxic lymphocyte granule constituents *in vitro* and *in vivo*. *Curr Opin Immunol* 2000; **12**: 323–9.

Available online at www.sciencedirect.com
SCIENCE DIRECT
Virology 352 (2006) 100–109
VIROLOGY
www.elsevier.com/locate/yviro

Expression of Kaposi's sarcoma-associated herpesvirus-encoded K10/10.1 protein in tissues and its interaction with poly(A)-binding protein

Takayuki Kanno, Yuko Sato, Tetsutaro Sata, Harutaka Katano *

Department of Pathology, National Institute of Infectious Diseases, 1-23-1 Toyama, Shinjuku-ku, Tokyo 162-8640, Japan

Received 12 December 2005; returned to author for revision 6 January 2006; accepted 5 April 2006
Available online 22 May 2006

Abstract

The K10/10.1 protein is encoded by a cluster of interferon regulatory factor (IRF) homologues in the Kaposi's sarcoma-associated herpesvirus (KSHV, human herpesvirus 8, HHV-8) genome. In the present study, we showed that an anti-K10 antibody reacted with a 110-kDa protein encoded by the K10/10.1 gene of KSHV in KSHV-infected primary effusion lymphoma (PEL) cell lines. Expression of K10/10.1 protein was induced by phorbol ester in KSHV-infected cells. A reporter gene assay demonstrated that K10/10.1 protein did not influence promoter activity of human interferon genes, regardless of its homology to human IRFs. Poly(A)-binding protein (PABP) was identified as a partner of K10/10.1 protein. Immunoprecipitation revealed that K10/10.1 protein interacted with PABP specifically in PEL cell lines. IFA revealed co-localization of K10/10.1 protein and PABP in the nucleus of KSHV-infected cells. These data suggest that K10/10.1 protein may affect the translational status or stability of mRNA in host cells.

Keywords: Kaposi's sarcoma-associated herpesvirus (KSHV/HHV-8); K10/10.1; Kaposi's sarcoma (KS); Multicentric Castleman's disease (MCD); Poly(A)-binding protein (PABP); Primary effusion lymphoma (PEL)

Introduction

Kaposi's sarcoma-associated herpesvirus (KSHV, human herpesvirus 8, HHV-8) is associated with the pathogenesis of KS, primary effusion lymphoma (PEL), and multicentric Castleman's disease (MCD) (Moore and Chang, 2001). One of the unique characteristics of this virus is that it encodes several homologues of human cytokines, cell cycle-associated genes, and chemokines. Among them, KSHV contains a cluster of interferon regulatory factor (IRF)-encoded genes in its genome. At least 7 homologues of IRFs have been identified in this cluster, i.e., K9 (viral IRF-1 or vIRF-1), K10, K10.1 (vIRF-4), K10.5 (vIRF-3 or LANA2), K10.7, K11, and vIRF2 (Afonina et al., 1998; Burysek et al., 1999; Cunningham et al., 2003; Lubyova and Pitha, 2000; Rivas et al., 2001). Some of these IRF homologues have been previously investigated, and their functions have been reported. vIRF-1 was found to have a similar function to human IRF-2 (hIRF-2) (Burysek et al., 1999; Li et al., 1998; Pozharskaya et al., 2004; Zimring et al., 1998). Like hIRF-2, vIRF-1 suppresses type I-interferon promoter activity and IFN-stimulated activation of IFN-stimulated gene (ISG) promoters (Afonina et al., 1998; Burysek et al., 1999; Zimring et al., 1998). vIRF-1 is also involved in oncogenesis by binding cellular p53 and CBP/p300 (Burysek et al., 1999). vIRF-2 suppresses interferon promoter activity and binds to IRF-1, IRF-2, ICSBP, and CBP (Burysek and Pitha, 2001; Burysek et al., 1999). vIRF-2 interacts with double-stranded RNA-activated protein kinase and inhibits antiviral effects of interferon (Burysek and Pitha, 2001). vIRF-3 (LANA2) is unique among vIRFs (Lubyova et al., 2004; Lubyova and Pitha, 2000; Rivas et al., 2001). Its kinetics are those of the latent proteins, and almost all KSHV-infected B-cells express vIRF-3 in their nucleus (Rivas et al., 2001). Moreover, vIRF-3 inhibits p53-dependent apoptosis by binding to p53 and CBP/p300, suggesting that vIRF-3 plays an important role in pathogenesis of malignancies with a latent infection with KSHV (Lubyova et al., 2004; Rivas et al., 2001). Thus, KSHV-encoded IRFs show

* Corresponding author. Fax: +81 3 5285 1189.
E-mail address: katano@nih.go.jp (H. Katano).

0042-6822/$ - see front matter © 2006 Elsevier Inc. All rights reserved.
doi:10.1016/j.virol.2006.04.009

various functions, and their expression varies among genes. On the other hand, other vIRFs, e.g., K10, K11, vIRF4 (K10.1), and K10.7, have been poorly characterized, and their functions are still unknown (Cunningham et al., 2003). We previously showed that expression of K10 protein was induced by 12-*O*-tetradecanoylphorbol-13-acetate (TPA) in the KSHV-infected PEL cell lines, suggesting that K10 protein belonged to a family of lytic proteins (Katano et al., 2000b). Histologically, K10 protein is expressed in the nucleus by very few tumor cells in Kaposi's sarcoma (KS) tissues, although a small number of mantle zone B cells express K10 protein in their cytoplasm in multicentric Castleman's disease (MCD) tissues (Katano et al., 2000b). Furthermore, the length of ORF K10 gene is more than 2 kbp, which makes it the longest gene among all vIRFs (Cunningham et al., 2003). Transcriptional analysis revealed that ORF K10 was transcribed with ORF K10.1 as a fusion gene (K10/10.1 gene) (Cunningham et al., 2003; Jenner et al., 2001). Even though a part of the K10 gene is homologous to hIRFs, a large part of it does not correspond to any other human genes. Therefore, we hypothesized that K10/10.1 protein, a product of K10/10.1 gene, had other functions besides those of IRFs. In the present study, we revealed that the K10/10.1 transcript produced a 110-kDa protein (K10/10.1 protein), and we identified poly (A)-binding protein as a binding partner of the K10/10.1 protein.

Results

Cloning of the K10/10.1 transcript from a cDNA library

To identify transcripts encoded by the K10 gene, we immunoscreened a cDNA library. When 1×10^6 clones of a cDNA library constructed from TY-1 cells were screened using the anti-K10 polyclonal antibody (Katano et al., 2000b), 8 positive clones were obtained. Sequence analysis revealed that these clones consisted of 3 groups. The first group contained a 2921-bp cDNA with a poly(A) signal sequence corresponding to the K10/10.1 transcript (Jenner et al., 2001). The 2 other clone groups were shorter than the K10/10.1 group, and only coded for the K10 gene characterized as a 2281-bp fragment (bases 88,286–86,006 of GenBank acc. no. U75698) or a 2080-bp fragment (bases 88,085–86,006 of GenBank acc. no. U75698). To confirm expressions of these three forms of K10 transcripts, we performed Northern blot hybridization using the K10 gene as a probe. Northern blotting demonstrated that two bands were induced in TY-1 cells with TPA stimulation (Fig. 1A). The size of the longest band was 2.9 kb, possibly corresponding to the K10/10.1 transcript (Jenner et al., 2001). No band was found at 2281 and 2080 b. In addition to the band of the K10/10.1 transcript, a strong 1.0-kb band was observed in stimulated PEL cells, suggesting the presence of another form of the K10 gene. Unstimulated PEL cells demonstrated two

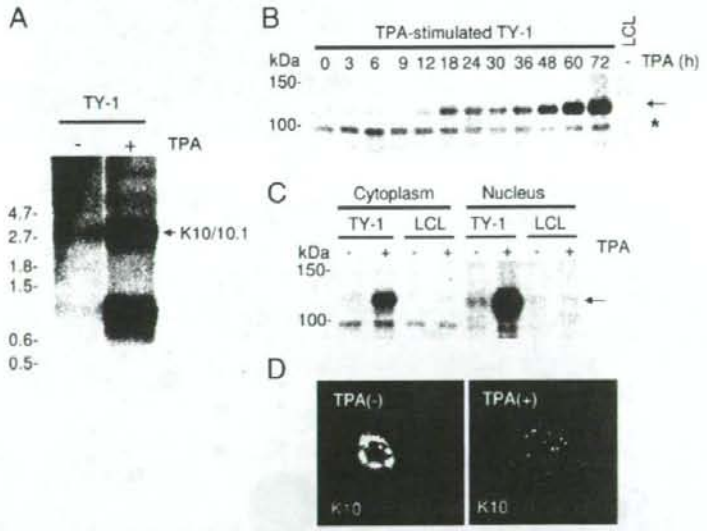

Fig. 1. Expression of K10/10.1 gene and protein in a PEL cell line. (A) Northern blot hybridization. mRNAs extracted from TPA-stimulated TY-1 (+) or unstimulated TY-1 (−) cells were electrophoresed and blotted on a membrane. Radiolabeled K10 DNA (amplified by PCR) was used as probe. The arrow indicates the K10/10.1 gene transcript. The lower band at 1.0 kb represents another transcript of the K10 gene. (B) Western blot analysis for K10/10.1 protein in TPA-stimulated TY-1 cells. Numbers of hours after addition of TPA are shown at the top of the panel. LCL: lymphoblastoid cell line as a negative control. The arrow indicates specific bands obtained with the anti-K10 rabbit polyclonal antibody, while lower bands (asterisk) are non-specific. (C) Western blot analysis for K10/10.1 protein in subcellular fractions. The arrow indicates K10/10.1 protein-specific bands. (D) IFA of K10/10.1 protein in unstimulated (left) and TPA-stimulated TY-1 (right) cells using anti-K10 rabbit polyclonal antibody. K10/10.1 protein is represented in green color. The red color indicates nuclear counterstaining with propidium iodide.

weak bands at 2.9 kb and 1.0 kb. Thus, we concluded that a 2.9-kb transcript of K10/10.1 was the major transcript of the K10/10.1 gene, and that 2 other short clone groups were artificially present.

Expression and kinetics of K10/10.1 gene/protein in PEL cell lines

Several studies reported kinetics of KSHV-encoded genes in PEL cell lines (Fakhari and Dittmer, 2002; Jenner et al., 2001; Sun et al., 1999). We previously demonstrated that K10 protein was induced by TPA, suggesting that K10 protein was a lytic protein (Katano et al., 2000b). DNA array analysis by another group suggested the presence of 2 transcripts including the K10 gene, i.e., K10/10.1 and K10 (Jenner et al., 2001). Cluster analysis and RT-PCR suggested that K10 might be a latent gene, whereas K10/10.1 was a lytic gene (Jenner et al., 2001). Thus, we examined expressions of K10/10.1 gene and protein in PEL cell lines. Northern blot analysis demonstrated that K10/10.1 transcript (2.9 kb) was induced by TPA in TY-1 cells (Fig. 1A). Western blotting demonstrated that an anti-K10 antibody reacted with a 110-kDa protein of K10/10.1, and that amount of K10/10.1 protein increased after addition of TPA (Fig. 1B). Subcellular fractionation revealed that K10/10.1 protein was expressed mainly in the nucleus, and partly in the cytoplasm (Fig. 1C). IFA using anti-K10 antibody showed that K10/10.1 protein was expressed in the nucleus of a very small population of unstimulated PEL cells (Fig. 1D). When stimulated with TPA, the number of K10/10.1-positive cells increased. Dot-like signals were observed not only in the nucleus, but also in the cytoplasm of TPA-stimulated TY-1 cells (Fig. 1D). In addition, most of K10/10.1-positive cells expressed K10/10.1 protein in the nucleus, while some cells expressed K10/10.1 both in the cytoplasm and the nucleus. We also examined another KSHV-infected PEL cell line, BCBL-1, and obtained similar results (data not shown).

Expression of K10/10.1 protein in KS, MCD, and KSHV-associated solid lymphoma

We previously developed a polyclonal antibody to K10 protein, and reported expression of K10 protein in KS and MCD tissues (Katano et al., 2000b). As we showed in Fig. 1, Western blot analysis revealed that this anti-K10 antibody reacted with K10/10.1 protein predominantly (Fig. 1). In order to further reveal the detailed expression of K10/10.1 protein in KSHV-associated diseases, we performed immunohistochemistry for K10/10.1 protein in additional cases of KS, MCD, and in an animal model of KSHV-associated solid lymphoma (Katano et al., 2000b). As it was previously reported (Katano et al., 2000b),

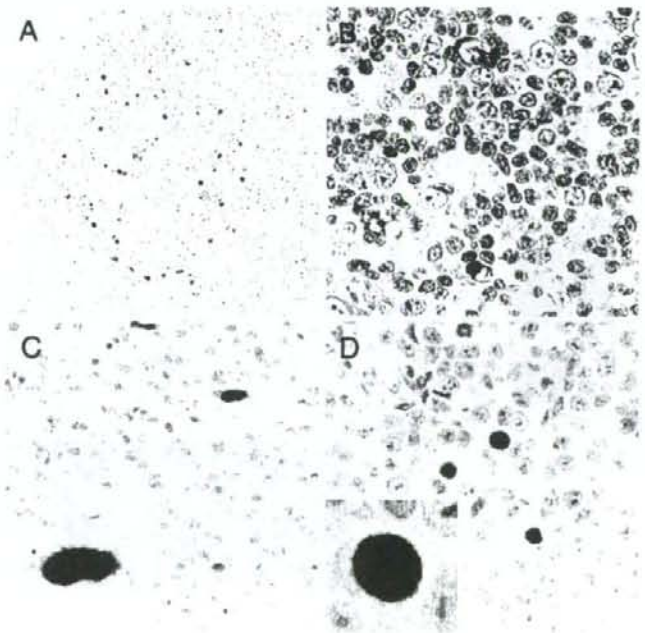

Fig. 2. Immunohistochemistry of K10/10.1 protein in KSHV-associated diseases. (A and B) Lymph node from a patient with MCD. The low power view shows K10/10.1 protein-positive cells in the mantle zone of the germinal center in a MCD lesion (A). Some B cells in the mantle zone show positive signals in the cytoplasm (B). (C) Kaposi's sarcoma (KS). One cell expresses K10/10.1 protein in this panel. In the high power view, diffuse staining is present in the nucleus (inset). (D) An animal model of KSHV-associated solid lymphoma. Some of the lymphoma cells are positive for K10/10.1 protein. In the high power view, the signal is seen as a dot-like staining pattern in the nucleus (inset).

we found that K10/10.1 protein was expressed predominantly in the cytoplasm of B cells in the mantle zone of MCD lesions (Figs. 2A and B). Expression of K10/10.1 protein was observed in the nucleus of KS cells, and the frequency of K10/10.1-positive cells was very low (less than 1%) in KS lesions (Fig. 2C). In an animal model of KSHV-associated solid lymphoma, K10/10.1 protein was expressed in the nucleus of lymphoma cells (Fig. 2D). A careful observation revealed that staining with the anti K10 antibody showed a dot-like pattern in the nucleus (Fig. 2D, inset).

Localization of K10/10.1 in transfectants

To investigate function and expression of K10/10.1 protein, we constructed a plasmid expressing K10/10.1 protein. A transfection study demonstrated that the expression plasmid produced a 110-kDa protein that reacted with anti-K10 antibody in 293T cells (Fig. 3A). IFA revealed its subcellular localization in K10/10.1-transfected HeLa cells (Fig. 3B). While K10/10.1 protein was expressed predominantly in the nucleus in 30% of transfectants, 60% of transfected cells expressed K10/10.1 protein in both the cytoplasm and nucleus, and the remaining 10% of cells showed K10/10.1 protein predominantly in the cytoplasm. We next constructed GFP-tagged plasmids expressing the K10/10.1 protein, and transfected them into HeLa cells (Fig. 3C). Similar localization was observed in the GFP-K10/10.1-transfected HeLa cells. Although PROSITE, an online protein domain searchable database (http://us.expasy.org/prosite/), did not detect any putative sequence of nuclear localization signals in the K10/10.1 gene, our data suggested that K10/10.1 might have unknown nuclear localization signals or DNA binding domains.

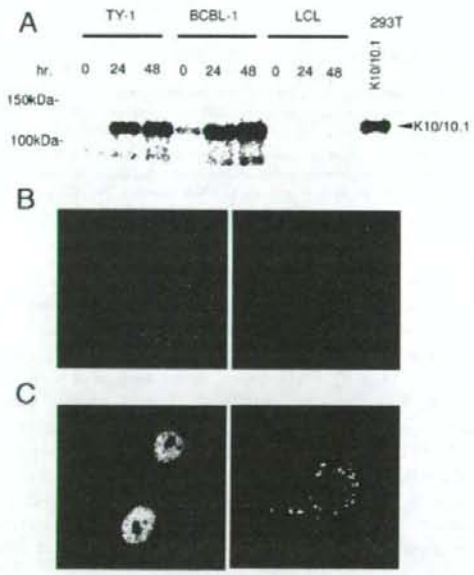

Fig. 3. Expression of K10/10.1 transcript in transfectants. (A) Western blot analysis. In 293T transfectants, the K10/10.1 transcript produced a protein with a similar size to that of K10/10.1 proteins in KSHV-infected PEL cell lines. (B) Localization of each form of K10 proteins in HeLa cells. The red color indicates K10/10.1 protein, and the blue color is the nucleus (TOPRO3). K10/10.1 protein is present predominantly in the nucleus (left panel) and rarely in the cytoplasm (right panel). (C) Localization of GFP-K10/10.1 protein in HeLa cells. GFP signal is observed predominantly in the nucleus (left panel), sometimes in both the cytoplasm and nucleus (right panel).

Functions as a homologue of IRFs

Since the K10/10.1 transcript is encoded in the cluster of vIRFs in KSHV genome, we compared the K10/10.1 protein with IRFs using multiple sequence alignments with the Clustal X software. Multiple sequence alignments demonstrated that K10.1 (the N-terminal region of the K10/10.1 protein) coded homologous regions to the DNA binding domain of IRFs, including a tryptophan pentad repeat (Fig. 4A). The N-terminus of the K10 protein, which localized in a middle part of K10/10.1 protein, also showed homologous regions to the DNA binding domain of IRFs. Moreover, K10/10.1 protein has some homologous regions in its C-terminus. A phylogenic tree analysis revealed that both K10 and K10.1 belonged to the same cluster as vIRF-1, suggesting that K10/10.1 protein might have similar functions to IRFs (Fig. 4B).

IFA demonstrated a dot-like staining pattern in the nucleus of PEL cell lines (Fig. 1D). It is known that vIRF-1 localizes in the promyelocytic leukemia protein (PML) bodies in the nucleus (Pozharskaya et al., 2004). Since K10/10.1 protein has a homology to vIRF-1, we investigated whether K10/10.1 protein co-localized with the PML bodies. IFA demonstrated that staining of K10/10.1 protein only partially overlapped with that of PML (Fig. 4C). Some hIRFs co-localize with the SC35 domain, a component in the nucleus close to the PML bodies (Maul, 1998). Therefore, we investigated if K10/10.1 protein co-localized with SC35. IFA revealed that signals of K10/10.1 protein overlapped with those of SC35 (Fig. 4D), suggesting that K10/10.1 protein was expressed in the SC35 domain near the PML body in the nucleus.

We then examined if K10/10.1 protein suppressed promoter activity of interferons. A reporter gene assay using pGL3-IFNB-Luc demonstrated that K10/10.1 protein did not suppress promoter activity of IFNB induced by a Sendai virus infection (Fig. 4E). These data suggested that K10/10.1 protein might not suppress promoter activity of IFNs, while K10/10.1 protein shows some homology with IRFs.

PABP binds to K10/10.1 protein

To further clarify the function of K10/10.1 protein, we next investigated its binding protein. GST-K10 fusion protein was mixed with TY-1 cell lysate, and a GST pull down assay was performed. SDS-PAGE of the pulled down proteins demonstrated the presence of a protein that specifically bound to K10 protein but not to GST in the TY-1 lysate (Fig. 5A). We excised the appropriate band from the gel, and analyzed it using matrix-

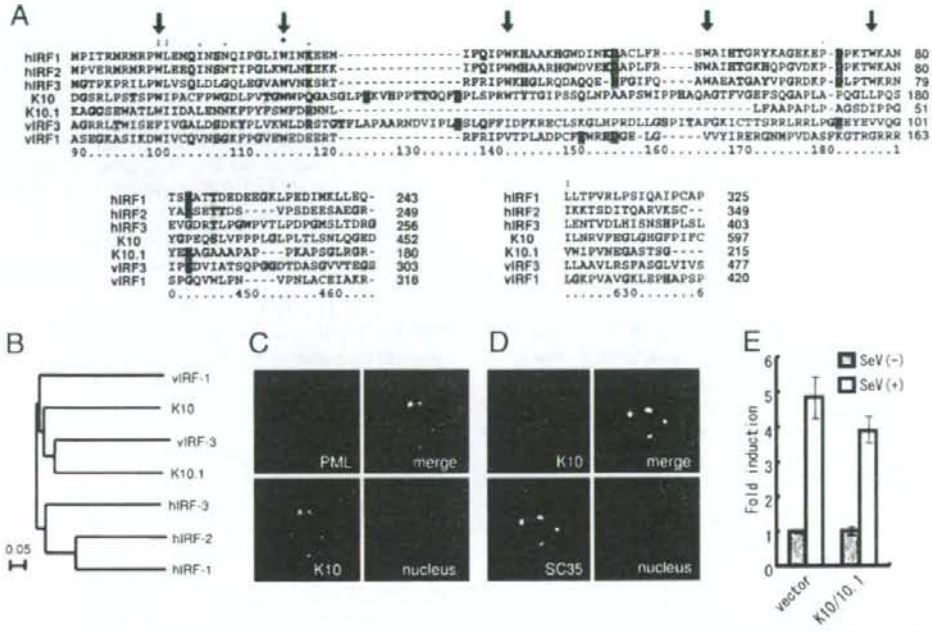

Fig. 4. K10/10.1 protein shows homologous domains to human and viral IRFs, but does not inhibit interferon promoter. (A) Alignment with IRFs using the Clustal X software. hIRF-1 (GenBank accession no. 87992), hIRF-2 (539621), hIRF-3 (4504725), vIRF-3 (AY008303), K10.1 (from 88410 to 88910 of KSU75698), K10 (from 86074 to 88164 of KSU75698), and vIRF-1 (4929348) were aligned. Arrows indicate tryptophan pentad repeats of the DNA binding domain. Numbers in the right of each panel indicate amino acids of each protein. Numbers counted automatically by the Cluster X were shown in the bottom of each panel. (B) Phylogenic tree analysis of IRFs, K10 and K10.1 proteins. The length of each branch indicates genetic distance with a scale size of 0.05 (5%). (C) Immunofluorescence of K10/10.1 protein and PML in TPA-stimulated TY-1 cells. PML and K10/10.1 protein were stained with Alexa 568 (red, upper left panel) and Alexa 488 (green, lower left panel), respectively. The nucleus was counterstained with TOPRO3 (blue, lower right panel). In the merged image (upper right), overlapping of the three colors is shown in white color. (D) Immunofluorescence of K10/10.1 protein and SC35 in TPA-stimulated TY-1 cells. (E) Reporter gene assay of IFNB promoter. The pGL3-IFNB-Luc reporter plasmid was co-transfected into HeLa cells with pBK-CMV vector (vector) and K10/10.1 expression plasmids. Cells were infected with Sendai virus 24 h after transfection, for 16 h, and analyzed for Luc activity. Error bars show standard deviation for triplicate experiments.

assisted laser desorption ionization/time-of-flight (MALDI-ToF) mass analysis. Mass spectrometry revealed that the protein corresponded to human poly(A)-binding protein (PABP), cytoplasmic 1. To confirm the binding of PABP to GST-K10 protein, we performed immunoblot analysis of the lysate obtained in the GST pull down (Fig. 5B). PABP was detected in the lysate pulled down with GST-K10 protein in the TY-1 lysate. In addition, Western blotting demonstrated that PABP was detected in the lysate immunoprecipitated with anti-K10 antibody in TY-1 and BCBL-1 cells (Fig. 5C). Moreover, K10/10.1 protein was detected in the lysate immunoprecipitated with anti-PABP antibody in cells (Fig. 5D). These data suggested that PABP bound to K10/10.1 protein in KSHV-infected PEL cells. To identify the binding site of PABP in K10/10.1 protein, we constructed plasmids expressing various deletion mutants of K10/10.1 protein (Fig. 6A). Immunoprecipitation clearly demonstrated that PABP bound to a 157–380 amino acid region of K10/10.1 protein (Fig. 6B). Finally, we investigated co-localization of PABP and K10/10.1 protein in KSHV-infected cells. In KSHV-infected PEL cells, TPA-stimulation induced K10/10.1 expression in the nucleus and cytoplasm (Fig. 1D). Interestingly, IFA revealed that PABP co-localized with K10/10.1 protein predominantly in the nucleus, but not in the cytoplasm (Fig. 7). Furthermore, in the nucleus of some cells, both K10/10.1 protein and PABP showed dot-like staining patterns, and co-localized in these dots. Since PABP localizes in the SC35 domain close to the PML bodies, and binds to poly(A) RNA in the nucleus (Afonina et al., 1998), these data suggested that K10/10.1 protein and PABP co-localized in the SC35 domain of TY-1 cells, and K10/10.1 protein might play a role in the function of PABP in the nucleus of KSHV-infected cells.

Discussion

In the present study, we characterized KSHV-encoded K10/10.1 protein. Our results showed that K10/10.1 protein was rarely expressed in the nucleus of KS cells, but was frequently found in the cytoplasm of the mantle zone B cells in MCD lesions. While functions of K10/10.1 protein are still unclear, K10/10.1 protein was identified as the longest homologue to

vIRFs, and its gene contained long sequences with no homology to IRFs. Thus, it is possible that K10/10.1 protein may have different functions from those of other vIRFs or hIRFs. Specifically, we showed that K10/10.1 protein did not influence promoter activity of interferons, and binding of K10/10.1 protein to PABP suggested that K10/10.1 protein affected host translation. Thus, K10/10.1 protein may play a different role from those of other viral IRFs in KSHV pathogenesis, while the K10/10.1 gene is encoded in the cluster of viral IRFs.

Although KSHV has been detected in KS, lymphoma, and MCD, association with KSHV differs among these KSHV-associated diseases (Katano et al., 2000b, Moore and Chang, 2001). We previously revealed that almost all KS cells expressed only latent gene products, and expression of lytic proteins was rare (Katano et al., 2000b). On the other hand, various lytic proteins encoded by KSHV, e.g., vIL-6, ORF59, and K8, have been detected in MCD lesions. These observations strongly suggested that lytic replication of KSHV was crucial in pathogenesis of MCD, whereas latency of KSHV was crucial in KS cells. Results of our immunohistochemical experiments demonstrated different subcellular localizations of K10/10.1 protein between KS and MCD. This differential subcellular localization of K10/10.1 protein was also observed between unstimulated and TPA-stimulated KSHV-infected PEL cell lines. Cytoplasmic localization of K10/10.1 protein was observed only in TPA-stimulated cells. Therefore, cytoplasmic staining of K10/10.1 protein in MCD lesions suggested that B cells in the mantle zone would be in the lytic phase of KSHV infection in MCD. Other KSHV-encoded proteins such as ORF59 demonstrated different subcellular localizations between unstimulated and TPA-stimulated TY-1 or BCBL-1 as well as between KS and MCD (unpublished data). However, expression of K10/10.1 protein demonstrated a very clear difference in MCD compared with that of ORF59. Therefore, it is possible that an anti-K10 antibody will provide a useful tool for the diagnosis of KSHV-associated MCD.

PABP is a multifunctional protein and is an important molecule for mRNA stabilization, translation initiation, protection of poly(A) from nuclease activity, mRNA deadenylation, and mRNP maturation in host cells (Grosset et al., 2000; Guhaniyogi and Brewer, 2001; Minvielle-Sebastia et al., 1997). In particular, PABP may play an important role in regulating mRNA turnover by inhibiting mRNA decapping with its poly (A)-tail (Khanna and Kiledjian, 2004). PABP is predominantly present in the cytoplasm, although it is also found in the nucleus (Afonina et al., 1998). A study using GFP-tagged PABP revealed that PABP shuttled between the cytoplasm and the nucleus (Afonina et al., 1998). In the nucleus, PABP predominantly co-localizes with SC35, a splicing factor, and interacts with the poly(A)-tail (Afonina et al., 1998). It is also known that SC35 is localized close to the PML bodies in the nucleus (Maul, 1998). In the present study, immunoprecipitation suggested that a limited amount of K10/10.1 protein actually bound to PABP in KSHV-infected cells (Figs. 5C and D). IFA

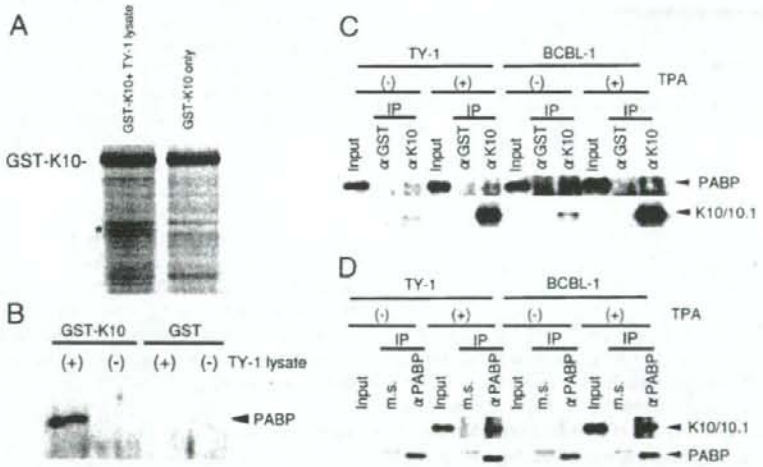

Fig. 5. K10/10.1 protein binds to PABP. (A) GST pull down assay. Ten micrograms of GST-K10 protein was incubated with TY-1 cell lysate. After adding glutathione–Sepharose beads, the beads were washed 3 times with lysis buffer. Then, the beads were loaded for SDS-PAGE using 2× sample buffer. The gel was stained with Coomassie brilliant blue. The asterisk indicates a band observed only in the lane of GST-K10 protein + TY-1 lysate, and not in the GST-K10 protein lane; as well as not in the GST protein + TY-1 lysate lane and the GST protein only lane (data not shown). (B) Western blotting of GST pulled down lysates. Beads obtained from the GST pull down assay were electrophoresed using SDS-PAGE, and blotted on a membrane. The membrane was stained with anti-PABP antibody. (C) Immunoprecipitation (IP) with anti-K10 antibody and immunoblotting with PABP. Lysates from TY-1 and BCBL-1 were immunoprecipitated with anti-K10 antibody or anti-GST antibody. Recombinant protein A-Sepharose was added and incubated. Sepharose was electrophoresed and blotted. Anti-PABP antibody was used as primary antibody for immunoblotting. Input indicates the whole lysate of TY-1 or BCBL-1 without IP. In the lower panel, anti-K10 antibody was used as primary antibody on the same membrane after stripping. (D) Immunoprecipitation with anti-PABP antibody and immunoblotting with anti-K10 antibody. Lysates from TY-1 and BCBL-1 were immunoprecipitated with anti-PABP antibody or normal mouse serum (m.s.). In the immunoblot, anti-K10 antibody was used as primary antibody for immunoblotting. In the lower panel, anti-PABP antibody was used as primary antibody on the same membrane after stripping.

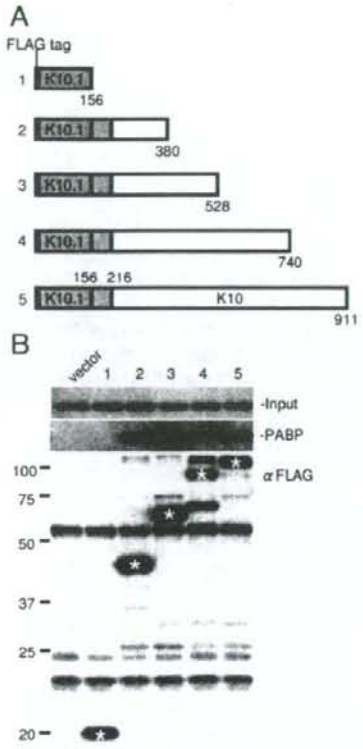

Fig. 6. Identification of the binding site of K10/10.1 protein with PABP. (A) Constructs of FLAG-tagged deletion mutants. K10/10.1 protein is composed of 911 amino acids. Four deletion mutants and a full-length K10/10.1 protein were constructed. (B) Immunoprecipitation. K10/10.1 mutants were immunoprecipitated with anti-FLAG antibody and were separated by SDS-PAGE. Endogenous PABP was detected in the top panel. Co-precipitated PABP with mutants are shown in the middle panel. Numbers on the top of the panel correspond to those in panel A. The lower panel shows sizes of deletion mutants by immunoblot using anti-FLAG antibody. Each band of mutant is indicated by white asterisks.

showed that K10/10.1 protein co-localized with PABP only in the nucleus (Fig. 7), whereas both PABP and K10/10.1 protein were present in the nucleus and cytoplasm. This might be one of the reasons why a limited amount of K10/10.1 protein bound to PABP. Overall, we can conclude that PABP forms a large complex near the PML bodies in the nucleus with SC35 and K10/10.1 protein, and is associated with mRNA turnover. It is known that some viral proteins such as poliovirus 3C protease and enterovirus proteases bind to, and cleave PABP, shutting off host translation (Joachims et al., 1999; Kuyumcu-Martinez et al., 2004). We investigated the amount of PABP in K10/10.1-transfected cells, but failed to detect changes in PABP expression levels (Kanno et al., unpublished data). Thus, K10/10.1 protein did not, at least in transfected cells, seem to directly alter PABP amount. However, our results suggested that K10/10.1 protein might inhibit function of PABP predominantly in the nucleus, resulting in shutoff of host translation. In KS cells, chemotherapy regimens including doxorubicin, bleomycin, and vincristine dramatically reduce amounts of cytoplasmic PABP, resulting in translation shutoff and G2 arrests in host cells (van der Kuyl et al., 2002). Further studies are required to clarify relationships between K10/10.1 protein and PABP.

Materials and methods

Cell culture

KSHV-harboring TY-1 cells (Katano et al., 1999b) and BCBL-1 cells (AIDS Research and Reference Reagent Program #3233, National Institutes of Health, Bethesda, MD) were cultured in RPMI 1640, in the presence of 10% FCS. HeLa and 293T cells were cultured in DMEM with 10% FCS.

Immunoscreening

A cDNA library was constructed from TPA-stimulated TY-1 cells and a KSHV-infected cell line, using *Eco*RI-predigested lambda ZAP Express vectors according to the manufacturer's instructions (Stratagene, La Jolla, CA). Immunoscreening was performed as described previously (Katano et al., 1999a). Approximately 1×10^6 phages were screened on nitrocellulose filters using an anti-K10 polyclonal antibody (Katano et al., 2000b). The antibody was diluted 1:2000 in 1 × Block Ace (Snow Brand Milk Products, Tokyo, Japan), and incubated with filters for 1 h at room temperature. Filters were washed in phosphate-buffered saline (PBS)-0.1% Tween 20, reacted with alkaline phosphatase-conjugated goat anti-rabbit immunoglobulin G (IgG, 1:5,000; Biosource), and visualized with nitroblue tetrazolium (NBT) and 5-bromo-1-chloro-3-indolylphosphate (BCIP, Promega, Madison, WI). Positive phages were selected, screened twice by the same protocol, and examined for their reactivity with the anti-K10 antibody. After conversion of positive phages into phagemids using the rapid excision system (Stratagene) and helper phages according to the manufacturer's instructions, inserts were sequenced with an ABI Prism 310 sequencer (Applied Biosystems, Foster City, CA) with the use of internal sequencing primers.

Northern blotting

Messenger RNA was extracted from TY-1 and BCBL-1 cells using a Fast Track 2.0 mRNA isolation kit (Invitrogen, Carlsbad, CA). Fifteen micrograms of mRNA were separated on 1% formaldehyde-containing agarose gel, transferred to a nylon filter, and hybridized with a probe. K10 PCR products (forward primer, 5′-CTCGGATCCCATCTACGTCCCCGTGGATA-3′; reverse primer, 5′-CTCGAATTCTGTAGATGCCGGGGATGCGC-3′; template DNA, TY-1 DNA; product size, 1767 bp) were labeled with ^{32}P (High Prime, Roche Applied Science, Mannheim, Germany), and used as probe.

Western blotting

Cell extract preparation and immunoblots were performed as described previously (Katano et al., 2001). Proteins were separated by sodium dodecyl sulfate-polyacrylamide gel electrophoresis (SDS-PAGE), probed with anti-K10 rabbit polyclonal antibody (Katano et al., 2000b) or anti-PABP mouse monoclonal antibody (ImmuQuest, Santa Cruz, CA), followed by incubation with horseradish peroxidase-conjugated anti-rabbit (or mouse) antibodies (Biosource International, Camarillo, CA), and visualization using ECL plus (Amersham Pharmacia Biotech, Buckinghamshire, UK).

Subcellular fractionation

Subcellular fractionation was prepared for TY-1 and LCL cells with/without TPA stimulation. 1×10^7 cells were lyzed in hypotonic buffer (20 mM HEPES pH 7.0, 10 mM KCl, 1 mM $MgCl_2$, 0.5 mM DTT, 0.1% Triton X-100) for 20 min on ice. After voltexing for 30 s, lysates were centrifuged at 13,000×*g* for 10 s. Supernatants were used as cytoplasmic fractions. Pellets were washed with hypotonic buffer twice, lyzed in extraction buffer (20% Glycerol, 420 mM NaCl, 20 mM HEPES pH 7.0, 10 mM KCl, 1 mM $MgCl_2$, 0.5 mM DTT, 0.1% Triton X-100), and centrifuged. Supernatants were used as nuclear extracts. A protease-inhibitor cocktail (Complete, EDTA-free, Roche Diagnostics, Indianapolis, IN) was added to the buffer before use.

Immunofluorescence assay (IFA)

IFA was performed as described previously (Katano et al., 2001). Anti-K10 (Katano et al., 2000b), PML (Santa Cruz Biotechnology, Santa Cruz, CA), SC35 (Sigma-Aldrich, St. Louis, MO), or PABP (ImmuQuest) antibodies were used as primary antibodies. Secondary antibodies were either Alexa-488 or Alexa-568 conjugated anti-rabbit (or anti-mouse) IgG antibodies (Molecular Probe, Eugene, OR). TOPRO3 (Molecular Probe) was used for counterstaining cell nuclei. Imaging was performed using a confocal microscope equipped with an argon-krypton laser (LSM-MicroSystem, Zeiss, Germany).

Immunohistochemistry

Formalin-fixed specimens of KS, MCD, and the animal model of KSHV-associated solid lymphoma were embedded in paraffin, sectioned, and stained with hematoxylin and eosin. Immunohistochemistry was performed with an anti-K10 rabbit polyclonal antibody (Katano et al., 2000b). For second and third phase reagents of immunostaining, a biotinylated F(ab')2 fragment of goat anti-rabbit immunoglobulin (DAKO, Copenhagen, Denmark) and peroxidase-conjugated streptavidin (DAKO) were used. Details regarding immunostaining methods have been described previously (Katano et al., 2000b). An animal model of KSHV-associated solid lymphoma was established as described previously (Katano et al., 2000c). Briefly, TY-1 cells were inoculated into the subcutaneous tissue of mice with severe combined immunodeficiency (SCID). One month after inoculation, lymphomas appeared in the subcutaneous region at the inoculation site. Lymphoma cells contained the KSHV genome and expressed various viral proteins of KSHV (Katano et al., 2000c).

Plasmids

Expression vectors of K10.10.1 were obtained using an in vivo excision system from phage plaques (Stratagene). To construct pEGFP-K10.10.1, the K10.10.1 gene was amplified by PCR using forward (5′-CTACTCGAGCCTAAAGCC-GGTGGCTCAGAATGG-3′) and reverse (5′-CGGGGATCCT-CAATGTAGACTATCCCAAATGGA-3′) primers from the expression plasmid. PCR products were cloned into the *Xho*I/*Bam*HI sites of pEGFP (BD Biosiences Clontech, Mountain

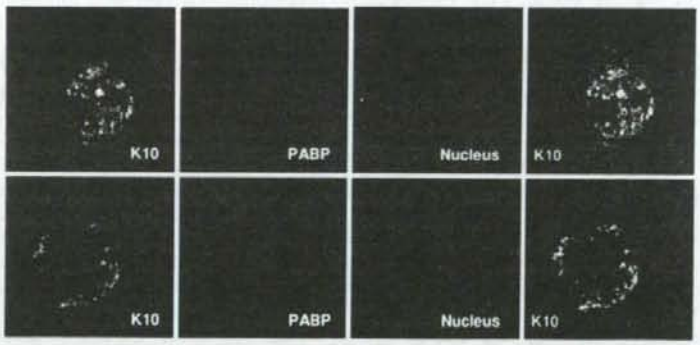

Fig. 7. IFA of TPA-stimulated TY-1 cells. K10.10.1 protein and PABP co-localize in the nucleus, but not in the cytoplasm. In some cells, K10.10.1 protein is present in the nucleus as a patchy pattern, and is diffusely distributed in the cytoplasm (upper panels). PABP co-localizes with K10.10.1 protein in the nucleus, as a patchy staining pattern in the upper panels. In the lower panels, K10.10.1 protein is expressed predominantly in the nucleus and co-localizes with PABP as a dot-like staining pattern near the nuclear membrane in the nucleus.

View, CA). For the reporter assay of interferon regulatory factors, pIFNB-Luc was constructed as reported previously (Lubyova et al., 2004). For constructions of deletion mutants, 5 fragments of K10/10.1 were amplified with PCR using one forward primer (5′-CTAGAATTCCCTAAAGCCGGTGGCTCAGAATGG-3′) and 5 reverse primers (5′-TAAGCGGCCGCTCAAACCTCACACCCCCTTC-3′ for amino acids no. 1–156, 5′-TAAGCGGCCGCTTAGAACTCACCGACAAATGTTCCCGC-3′ for amino acids no. 1–380, 5′-TAAGCGGCCGCTGGCTCCTGCGCTCTGCGACCTCT-3′ for amino acids no. 1–528, 5′-CGAGCGGCCGCTCAAAAGATTTCCACAACAAAAGACAC -3′ for amino acids no. 1–740, 5′-CATGCGGCCGCTCAATGTAGACTATCCCAAATGGA-3′ for full length of K10/10.1). PCR products were cloned into the *Eco*RI site of pME18FLAG (Ishida et al., 1996).

Transfection and luciferase assays

Expression plasmids were transfected into HeLa or 293T cells using Lipofectamine Plus (Invitrogen) for HeLa cells or Fugene 6 (Roche Diagnostics, Indianapolis, IN) for 293T cells, according to the manufacturer's instructions. An IFN promoter assay was performed as reported previously (Lubyova et al., 2004). Briefly, K10/10.1 expression plasmid and empty vector were co-transfected with pGL3-IFNB-Luc and phRL-CMV vector into HeLa cells with lipofectamine Plus (Invitrogen). Twenty-four hours after transfection, wells were washed, and Sendai virus was added to 1% BSA phosphate-buffered saline with a m.o.i of 5. Luciferase activity was measured using a dual luciferase assay system (Promega).

GST pull down assay

To identify the binding protein to K10/10.1 protein, a glutathione *S*-transferase (GST) pull down assay was performed. GST-K10 fusion gene was generated by ligation of a *Bam*HI–*Eco*RI-digested PCR product of the K10 gene to the *Bam*HI–*Eco*RI site of *p*GEX 5X-2 (Amersham Pharmacia Biotech) (Katano et al., 2000a). GST-K10 fusion protein was then expressed in *Escherichia coli*, and affinity-purified using glutathione–Sepharose as described previously (Katano et al., 2000a). Purity and concentration of eluted proteins were determined by SDS-PAGE and the Bradford assay (Protein Assay; BioRad, New York, NY), respectively. TY-1 cells (1×10^7) were washed with PBS and lyzed in 1 ml lysis buffer (50 mM Tris–HCl, pH 8.0, 150 mM NaCl, 0.1% SDS, 0.5% sodium deoxycholate, 0.5% Nonidet P-40, 1 mM phenylmethylsulfonyl fluoride, 100 U/ml aprotinin, and 0.02% sodium azide). After absorption of glutathione–Sepharose beads (Amersham Pharmacia Biotech), 10 μg GST-K10 protein or GST protein that was purified with a glutathione–Sepharose 4B column was added, and incubated at 4 °C for 2 h. Then, 25 μl glutathione–Sepharose beads were added, and incubated for 1 h. The beads were washed 3 times in carbonate buffer containing 100 mM $NaHCO_3$ and 300 mM NaCl. Bound proteins were eluted with an equal volume of 2× sampling buffer and separated by SDS-PAGE.

Mass spectrometry

Bands of interest were excised from Coomassie-stained gels, followed by destaining, reduction, alkylation, and digestion with modified porcine trypsin (Promega). Samples for MALDI-ToF analysis were prepared by mixing a small aliquot of the digested supernatant with an equal volume of a solution of alpha-cyano-4-hydroxycinnamic acid (10 mg/ml in 1:1 acetonitrile: 0.1% vol/vol trifluoroacetic acid). Peptide mass fingerprinting was performed on a reflectron MALDI-ToF mass spectrometer (Voyger, Amersham Biosciences). The Protein Prospector (http://prospector.ucsf.edu/) was employed for protein database search using monoisotopic mass values for each spectrum.

Immunoprecipitation

Cells (1×10^6) were lyzed in 1 ml lysis buffer (50 mM Tris–HCl, pH 8.0, 150 mM NaCl, 1% Nonidet P-40, 1 mM phenylmethylsulfonyl fluoride, 100 U/ml aprotinin, 1 mM DTT). After absorption of recombinant protein A–Sepharose (Amersham Pharmacia Biotech, Buckinghamshire, UK), equal amounts of cell lysates were incubated with equal amounts of a polyclonal antibody against the K10 protein or preimmune-rabbit serum. The proteins separated by SDS-PAGE were transferred onto membranes (Immobilon; Millipore, Bedford, MA).

Deletion mutants

Plasmids expressing mutant K10/10.1 were transfected in 293T cells. Transfectants were lyzed, and equal amounts of lysate were incubated with anti-FLAG M2 antibody (Sigma). Recombinant protein A-Sepharose was added, and proteins were separated by SDS-PAGE. Endogenous PABP was detected on a blotted membrane using anti-PABP antibody.

Acknowledgments

The authors would like to thank Dr. Atsushi Kato of the Department of Virology 3 at the National Institute of Infectious Diseases for providing Sendai virus samples, and Drs. Fumiko Shinkai-Ouchi and Yoshio Yamakawa of the Department of Biochemistry and Cell Biology at the National Institute of Infectious Diseases for their technical assistance on mass spectrometry. This research was supported by Health and Labor Sciences Research Grants on HIV/AIDS and Measures for Intractable Diseases from the Ministry of Health, Labor and Welfare (grants H15-AIDS-005 to H.K., and 17243601 to T.S.), a Grants-in-Aid for Scientific Research from the Ministry of Education, Culture, Sports, Science and Technology of Japan (grant 17590365 to H.K.), and a grant for Research on Health Sciences focusing on Drug Innovation from Japan Health Sciences Foundation (grant SA14831 to H.K).

References

Afonina, E., Stauber, R., Pavlakis, G.N., 1998. The human poly(A)-binding protein 1 shuttles between the nucleus and the cytoplasm. J. Biol. Chem. 273, 13015–13021.

Burysek, L., Pitha, P.M., 2001. Latently expressed human herpesvirus 8-encoded interferon regulatory factor 2 inhibits double-stranded RNA-activated protein kinase. J. Virol. 75, 2345–2352.

Burysek, L., Yeow, W.S., Lubyova, B., Kellum, M., Schafer, S.L., Huang, Y.Q., Pitha, P.M., 1999. Functional analysis of human herpesvirus 8-encoded viral interferon regulatory factor 1 and its association with cellular interferon regulatory factors and p300. J. Virol. 73, 7334–7342.

Cunningham, C., Barnard, S., Blackbourn, D.J., Davison, A.J., 2003. Transcription mapping of human herpesvirus 8 genes encoding viral interferon regulatory factors. J. Gen. Virol. 84, 1471–1483.

Fakhari, F.D., Dittmer, D.P., 2002. Charting latency transcripts in Kaposi's sarcoma-associated herpesvirus by whole-genome real-time quantitative PCR. J. Virol. 76, 6213–6223.

Grosset, C., Chen, C.Y., Xu, N., Sonenberg, N., Jacquemin-Sablon, H., Shyu, A.B., 2000. A mechanism for translationally coupled mRNA turnover: interaction between the poly(A) tail and a c-*fos* RNA coding determinant via a protein complex. Cell 103, 29–40.

Guhaniyogi, J., Brewer, G., 2001. Regulation of mRNA stability in mammalian cells. Gene 265, 11–23.

Ishida, T.K., Tojo, T., Aoki, T., Kobayashi, N., Ohishi, T., Watanabe, T., Yamamoto, T., Inoue, J., 1996. TRAF5, a novel tumor necrosis factor receptor-associated factor family protein, mediates CD40 signaling. Proc. Natl. Acad. Sci. U.S.A. 93, 9437–9442.

Jenner, R.G., Alba, M.M., Boshoff, C., Kellam, P., 2001. Kaposi's sarcoma-associated herpesvirus latent and lytic gene expression as revealed by DNA arrays. J. Virol. 75, 891–902.

Joachims, M., Van Breugel, P.C., Lloyd, R.E., 1999. Cleavage of poly(A)-binding protein by enterovirus proteases concurrent with inhibition of translation in vitro. J. Virol. 73, 718–727.

Katano, H., Hoshino, Y., Morishita, Y., Nakamura, T., Satoh, H., Iwamoto, A., Herndier, B., Mori, S., 1999a. Establishing and characterizing a CD30-positive cell line harboring HHV-8 from a primary effusion lymphoma. J. Med. Virol. 58, 394–401.

Katano, H., Sata, T., Suda, T., Nakamura, T., Tachikawa, N., Nishizumi, H., Sakurada, S., Hayashi, Y., Koike, M., Iwamoto, A., Kurata, T., Mori, S., 1999b. Expression and antigenicity of human herpesvirus 8 encoded ORF59 protein in AIDS-associated Kaposi's sarcoma. J. Med. Virol. 59, 346–355.

Katano, H., Iwasaki, T., Baba, N., Terai, M., Mori, S., Iwamoto, A., Kurata, T., Sata, T., 2000a. Identification of antigenic proteins encoded by human herpesvirus 8 and seroprevalence in the general population and among patients with and without Kaposi's sarcoma. J. Virol. 74, 3478–3485.

Katano, H., Sato, Y., Kurata, T., Mori, S., Sata, T., 2000b. Expression and localization of human herpesvirus 8-encoded proteins in primary effusion lymphoma, Kaposi's sarcoma, and multicentric Castleman's disease. Virology 269, 335–344.

Katano, H., Suda, T., Morishita, Y., Yamamoto, K., Hoshino, Y., Nakamura, K., Tachikawa, N., Sata, T., Hamaguchi, H., Iwamoto, A., Mori, S., 2000c. Human herpesvirus 8-associated solid lymphomas that occur in AIDS patients take anaplastic large cell morphology. Mod. Pathol. 13, 77–85.

Katano, H., Ogawa-Goto, K., Hasegawa, H., Kurata, T., Sata, T., 2001. Human-herpesvirus-8-encoded K8 protein colocalizes with the promyelocytic leukemia protein (PML) bodies and recruits p53 to the PML bodies. Virology 286, 446–455.

Khanna, R., Kiledjian, M., 2004. Poly(A)-binding-protein-mediated regulation of hDcp2 decapping in vitro. EMBO J. 23, 1968–1976.

Kuyumcu-Martinez, N.M., Van Eden, M.E., Younan, P., Lloyd, R.E., 2004. Cleavage of poly(A)-binding protein by poliovirus 3C protease inhibits host cell translation: a novel mechanism for host translation shutoff. Mol. Cell. Biol. 24, 1779–1790.

Li, M., Lee, H., Guo, J., Neipel, F., Fleckenstein, B., Ozato, K., Jung, J.U., 1998. Kaposi's sarcoma-associated herpesvirus viral interferon regulatory factor. J. Virol. 72, 5433–5440.

Lubyova, B., Pitha, P.M., 2000. Characterization of a novel human herpesvirus 8-encoded protein, vIRF-3, that shows homology to viral and cellular interferon regulatory factors. J. Virol. 74, 8194–8201.

Lubyova, B., Kellum, M.J., Frisancho, A.J., Pitha, P.M., 2004. Kaposi's sarcoma-associated herpesvirus-encoded vIRF-3 stimulates the transcriptional activity of cellular IRF-3 and IRF-7. J. Biol. Chem. 279, 7643–7654.

Maul, G.G., 1998. Nuclear domain 10, the site of DNA virus transcription and replication. BioEssays 20, 660–667.

Minvielle-Sebastia, L., Preker, P.J., Wiederkehr, T., Strahm, Y., Keller, W., 1997. The major yeast poly(A)-binding protein is associated with cleavage factor IA and functions in premessenger RNA 3'-end formation. Proc. Natl. Acad. Sci. U.S.A. 94, 7897–7902.

Moore, P.S., Chang, Y., 2001. In: Knipe, D.M., Howley, P.M. (Eds.), Kaposi's Sarcoma-Associated Herpesvirus, 4th ed. Lippincott Williams and Wilkins, Philadelphia.

Pozharskaya, V.P., Weakland, L.L., Zimring, J.C., Krug, L.T., Unger, E.R., Neisch, A., Joshi, H., Inoue, N., Offermann, M.K., 2004. Short duration of elevated vIRF-1 expression during lytic replication of human herpesvirus 8 limits its ability to block antiviral responses induced by alpha interferon in BCBL-1 cells. J. Virol. 78, 6621–6635.

Rivas, C., Thlick, A.E., Parravicini, C., Moore, P.S., Chang, Y., 2001. Kaposi's sarcoma-associated herpesvirus LANA2 is a B-cell-specific latent viral protein that inhibits p53. J. Virol. 75, 429–438.

Sun, R., Lin, S.F., Staskus, K., Gradoville, L., Grogan, E., Haase, A., Miller, G., 1999. Kinetics of Kaposi's sarcoma-associated herpesvirus gene expression. J. Virol. 73, 2232–2242.

van der Kuyl, A.C., van den Burg, R., Zorgdrager, F., Dekker, J.T., Maas, J., van Noesel, C.J., Goudsmit, J., Cornelissen, M., 2002. Primary effect of chemotherapy on the transcription profile of AIDS-related Kaposi's sarcoma. BMC Cancer 2, 21.

Zimring, J.C., Goodbourn, S., Offermann, M.K., 1998. Human herpesvirus 8 encodes an interferon regulatory factor (IRF) homolog that represses IRF-1-mediated transcription. J. Virol. 72, 701–707.

Jpn J Ophthalmol 2006;50:7–11
© Japanese Ophthalmological Society 2006

DOI: 10.1007/s10384-005-0376-x

LABORATORY INVESTIGATION

Human Herpesvirus-8 in Kaposi's Sarcoma of the Conjunctiva in a Patient with AIDS

Hiroshi Minoda[1], Norio Usui[2], Tetsutaro Sata[3], Harutaka Katano[3], Hiromi Serizawa[4], and Shinya Okada[4]

[1]Department of Ophthalmology, Tokyo Medical University, Tokyo, Japan; [2]Shinkawabashi Hospital, Kawasaki, Japan; [3]Department of Pathology, National Institute of Infectious Diseases, Tokyo, Japan; [4]Department of Pathology, Tokyo Medical University, Tokyo, Japan

Abstract

Purpose: To demonstrate human herpesvirus-8 (HHV-8) in Kaposi's sarcoma (KS) of the conjunctiva in a patient with acquired immunodeficiency syndrome (AIDS).

Methods: Clinical observation, pathologic findings of conjunctival specimens, immunohistochemical staining for HHV-8-specific antigen, polymerase chain reaction (PCR) analysis of HHV-8 DNA, and detection of specific antibody in patient's serum at appropriate times.

Results: In the conjunctival specimen, swollen endothelial-like cells were found with slit-like vessels. CD 31-positive cells were noted on the inner surface of the slit-like vessels, and HHV-8 latency-associated nuclear antigen was detected. The presence of HHV-8 DNA was demonstrated by PCR. Anti-HHV-8 antibody was found in the patient's serum.

Conclusions: This is the first case report in the ophthalmology literature that provides histological, DNA, and serological evidence that HHV-8 is involved in the pathogenesis of conjunctival KS. **Jpn J Ophthalmol** 2006;50:7–11 © Japanese Ophthalmological Society 2006

Key Words: AIDS, conjunctiva, human herpesvirus-8, Kaposi's sarcoma, latency-associated nuclear antigen

Introduction

Kaposi's sarcoma (KS) is a malignant vascular neoplasm originally reported as a local disease in elderly people of Mediterranean countries. With the increase in acquired immunodeficiency syndrome (AIDS) cases, KS has been reported to be the most frequent malignant tumor developing in AIDS patients, especially among homosexual men in the United States. In the early 1980s, 15%–20% of AIDS patients developed KS,[1] and one-third of the patients were homosexual.[2] About 2% of AIDS patients developed KS either in the eyelids or conjunctiva,[3] but such cases are extremely rare and no documentation is available.

In 1994, specific herpesvirus-like DNA sequences were found in KS lesions of an AIDS patient, suggesting that a novel gamma herpesvirus, homologous to Epstein-Barr virus, exists in KS.[4] Subsequently, the virus was named human herpesvirus-8 (HHV-8). Thereafter, a number of viral studies have been performed on KS. However, there is no report in the field of ophthalmology that provides direct evidence of the involvement of HHV-8 in ocular lesions. In this study, we examined and treated an AIDS patient with ocular KS and detected HHV-8-specific antigen and HHV-8 DNA in conjunctival tissue as well as HHV-8-specific antibody in the serum. We present the clinical findings of this case because ocular KS is very rare in Japan. This case report also provides direct evidence for the first time in the

Received: January 18, 2005 / Accepted: April 26, 2005
Correspondence and reprint requests to: Hiroshi Minoda, Department of Ophthalmology, Tokyo Medical University, 6-7-1 Nishishinjuku, Shinjuku-ku, Tokyo 160-0023, Japan
e-mail: damino@za.pial.jp

Jpn J Ophthalmol
Vol 50: 7–11, 2006

ophthalmological literature that HHV-8 is involved in ocular KS.

Case Presentation

A 33-year-old homosexual Japanese man visited a dentist on June 19, 1999 because of swelling of the gingiva since early June (Fig. 1). A blood test was positive for human immunodeficiency virus (HIV) antibody. He was hospitalized in Tokyo Medical University Hospital, owing to fever and dyspnea, on June 26. AIDS was diagnosed based on a decreased CD4+ cell count (4/μl) and remarkably lowered cell-mediated immunity. After admission, a dark purple eruption was recognized on his trunk in addition to the gingival lesion. On June 30, he complained of feeling foreign bodies in both eyes and pain in the right eye, and underwent ophthalmological examinations. Two dark red, flatly elevated lesions 4 mm in width were recognized on the conjunctiva of both lower lids, and pedunculate lesions 3–4 mm in width were observed in the whole lower part of the conjunctival fornix and the medial canthus. Partial hemorrhage was observed in these lesions (Fig. 2). Abrasion by the lesion while blinking was considered to have produced epithelial erosion of the cornea. No abnormal findings were observed in the medial or posterior segments of the eyes. Bilateral pleural effusion and infiltration in the right and left lower lung fields were recognized by both chest X-ray and computed tomography (CT) examination.

Pathological examinations of the gingival lesions and transbronchial-lung biopsy specimens revealed proliferation of spindle cells and some specimens with vascular cavities, and KS was diagnosed. Highly active antiretroviral therapy using sanilvudine, lamivudine, and indinavir was started on July 8 as an anti-HIV treatment. Systemic administration of foscavir (120 mg/kg per day) for KS was given simultaneously for 21 days, from July 9 to July 29, but no tumor reduction was recognized. Invasion of the sarcoma from the mouth into the larynx increased the risk of airway obstruction, and the remarkable growth of sarcoma in the lungs, skin, and eyelids necessitated administration of doxorubicin hydrochloride (20 mg/m^2), bleomycin hydrochloride (20 mg/m^2), and vincristine sulfate (2 mg/m^2) from July 28.

After the chemotherapy, gum swelling and eruption on the trunk were reduced, and regression of sarcoma in the lung was confirmed by chest X-ray and CT. Although sarcoma of the eyelid showed some reduction in size, on August 6 we surgically removed a lesion at the lower eyelid fornix with microscissors under local anesthesia, for the purpose of definitive diagnosis and treatment evaluation. Pathological examination and molecular biological study for HHV-8 were performed on the specimen. In addition, we collected serum during the episode to examine anti-HHV-8 antibody. No recurrence of sarcoma was observed in the eyelids until January 2005, but eruption on the trunk and sarcoma in other locations recurred repeatedly, and regressed after reuse of chemotherapy. However, the number of CD-4-positive cells has increased, and no recurrence of the eruptions has been observed since August 2001.

Materials and Methods

This study was approved by the Ethics Committee of Tokyo Medical University.

Histopathology

The surgically removed specimen (18 mm × 2 mm) was fixed in 10% formalin, and the paraffin sections were stained with hematoxylin and eosin (H&E).

Immunohistochemistry

The deparaffinized sections were immunostained by the labeled streptavidin–biotin method (Dako, Glostrup, Denmark) using anti-human CD 31 mouse monoclonal antibody for vascular endothelial cells (Dako).[3]

To identify HHV-8 in the tumor tissue, we used a rabbit antibody (PA1-73N)[4] to ORF 73 protein, which is a latency-associated nuclear antigen (LANA) expressed in the latent phase of HHV-8 infection. The 4-μm sections were deparaffinized by sequential immersion in xylene and ethanol, rehydrated in distilled water, and irradiated for 15 min in a microwave oven for antigen retrieval. Endogenous peroxidase activity was blocked by immersing the sections in a methanol/0.6% H_2O_2 solution for 30 min at room temperature. Affinity-purified PA1-73N antibody [diluted 1:3000 in phosphate-buffered saline (PBS)/5% bovine serum albumin] was then applied, and the sections were incubated overnight at 4°C. After washing in PBS twice, the second and third reactions and the amplification procedure were performed using a kit (Dako) according to the manufacturer's instructions. The signals were visualized using 0.2 mg/ml diaminobenzidine and 0.015% H_2O_2 in 0.05 mol/l Tris-HCl, pH 7.6. Double immunostaining for LANA was performed as described previously.[3]

DNA Isolation by Polymerase Chain Reaction

Polymerase chain reaction (PCR) analysis for HHV-8 DNA was performed on conjunctival tissues. An HHV-8 DNA-positive cell line (TY-1)[5] established from an HHV-8-related tumor (primary effusion lymphoma) found in an AIDS patient was used as positive control. An HHV-8 DNA-negative cell line established from human umbilical vascular endothelial cells (HUVEC) was used as negative control. Total DNA was extracted by proteinase K digestion and phenol–chloroform–isoamyl alcohol treatment, as used routinely. PCR for HHV-8 DNA using KSBam$_{33}$233 was performed as described previously.[4] The PCR products were electrophoresed in 2% agarose gels to identify the 233-bp